

DESY-24-134  
 TIF-UNIMI-2024-17  
 Edinburgh 2024/9  
 CERN-TH-2024-167

# Combination of aN<sup>3</sup>LO PDFs and implications for Higgs production cross-sections at the LHC

## The MSHT Collaboration:

Thomas Cridge<sup>1</sup>, Lucian A. Harland-Lang<sup>2</sup>, Jamie McGowan<sup>2</sup>, and Robert S. Thorne<sup>2</sup>

## The NNPDF Collaboration:

Richard D. Ball<sup>3</sup>, Alessandro Candido<sup>4</sup>, Stefano Carrazza<sup>5</sup>, Juan Cruz-Martinez<sup>4</sup>, Luigi Del Debbio<sup>3</sup>,  
 Stefano Forte<sup>5</sup>, Felix Hekhorn<sup>6,7</sup>, Giacomo Magni<sup>8,9</sup>, Emanuele R. Nocera<sup>10</sup>,  
 Tanjona R. Rabemananjara<sup>8,9</sup>, Juan Rojo<sup>8,9</sup>, Roy Stegeman<sup>3</sup>, and Maria Ubiali<sup>11</sup>

<sup>1</sup> Deutsches Elektronen-Synchrotron DESY, Notkestr. 85, 22607 Hamburg, Germany

<sup>2</sup> Department of Physics and Astronomy, University College London, London, WC1E 6BT, UK

<sup>3</sup> The Higgs Centre for Theoretical Physics, University of Edinburgh,  
 JCMB, KB, Mayfield Rd, Edinburgh EH9 3FD, Scotland

<sup>4</sup> CERN, Theoretical Physics Department, CH-1211 Geneva 23, Switzerland

<sup>5</sup> Tif Lab, Dipartimento di Fisica, Università di Milano and  
 INFN, Sezione di Milano, Via Celoria 16, I-20133 Milano, Italy

<sup>6</sup> University of Jyväskylä, Department of Physics, P.O. Box 35, FI-40014 University of Jyväskylä, Finland

<sup>7</sup> Helsinki Institute of Physics, P.O. Box 64, FI-00014 University of Helsinki, Finland

<sup>8</sup> Department of Physics and Astronomy, Vrije Universiteit, NL-1081 HV Amsterdam

<sup>9</sup> Nikhef Theory Group, Science Park 105, 1098 XG Amsterdam, The Netherlands

<sup>10</sup> Dipartimento di Fisica, Università degli Studi di Torino and  
 INFN, Sezione di Torino, Via Pietro Giuria 1, I-10125 Torino, Italy

<sup>11</sup> DAMTP, University of Cambridge, Wilberforce Road, Cambridge, CB3 0WA, United Kingdom

## Abstract

We discuss how the two existing approximate N<sup>3</sup>LO (aN<sup>3</sup>LO) sets of parton distributions (PDFs) from the MSHT20 and NNPDF4.0 series can be combined for LHC phenomenology, both in the pure QCD case and for the QCD $\otimes$ QED sets that include the photon PDF. Using the resulting combinations, we present predictions for the total inclusive cross-section for Higgs production in gluon fusion, vector boson fusion, and associated production at the LHC with  $\sqrt{s} = 13.6$  TeV (Run 3). For the gluon fusion and vector boson fusion channels, the corrections that arise when using correctly matched aN<sup>3</sup>LO PDFs with N<sup>3</sup>LO cross section calculations, compared to using NNLO PDFs, are significant, in many cases larger than the PDF uncertainty, and generally larger than the differences between the two aN<sup>3</sup>LO PDF sets entering the combination. The combined aN<sup>3</sup>LO PDF sets, MSHT20xNNPDF40\_an3lo and MSHT20xNNPDF40\_an3lo\_qed, are made publicly available in the LHAPDF format and can be readily used for LHC phenomenology.

# 1 Introduction

The two global determinations of parton distribution functions (PDFs) from the MSHT [1] and NNPDF [2] collaborations have been recently extended to approximate next-to-next-to-next-to-leading order (aN<sup>3</sup>LO), in Refs. [3] and [4] respectively. Both the MSHT and NNPDF aN<sup>3</sup>LO PDF sets have been subsequently enlarged to also include a photon PDF and mixed QED $\otimes$ QCD corrections to perturbative evolution [5, 6].

The inclusion of N<sup>3</sup>LO QCD corrections in the determination of these PDF sets is approximate in two different respects. First, N<sup>3</sup>LO perturbative evolution is only known approximately. Indeed, splitting functions are not known exactly, so an approximation to them must be constructed based on exact knowledge of the small- and large- $x$  behavior at higher perturbative orders (e.g. from resummation) and a finite set of Mellin moments [7–17]. Knowledge of N<sup>3</sup>LO splitting functions has progressed rapidly, with more Mellin moments being gradually published over the years. In fact, now [18, 19] the full set of Mellin moments up to  $N = 20$  is available for all elements of the splitting function matrix. Heavy quark transition matrix elements at  $\mathcal{O}(\alpha_s^3)$ , which are needed for massless perturbative evolution in a variable-flavor number scheme, are now also fully known, albeit only recently in complete form [20–30]. Hence N<sup>3</sup>LO perturbative evolution is known exactly for all practical purposes, as we shall discuss in somewhat more detail below.

Second, however, N<sup>3</sup>LO partonic cross-sections are only known for a subset of the processes used for PDF determination, namely massless deep-inelastic scattering (DIS) [31, 32] and the total Drell-Yan cross-section and on-shell rapidity distribution [33–37]. In particular, whereas the computation of the high  $Q^2$  limit of heavy quark structure functions was recently completed, permitting the determination of heavy quark transition matrix elements, the computation of corrections to DIS coefficient functions proportional to powers of  $\frac{m_h^2}{Q^2}$  of the heavy quark mass is beyond the current state of the art, as is the computation of fiducial N<sup>3</sup>LO corrections to hadronic processes, which are needed for a meaningful comparison to hadron collider data.

As a consequence, while approximate N<sup>3</sup>LO perturbative evolution is close to exact, knowledge of N<sup>3</sup>LO hard cross sections is limited. Moreover, massless DIS data do not fully determine the PDFs, and consequently a N<sup>3</sup>LO PDF determination must include a number of processes for which only NNLO matrix elements are available. It is in this respect that perturbative accuracy in aN<sup>3</sup>LO PDF determination is not fully N<sup>3</sup>LO.

The two available aN<sup>3</sup>LO PDF determinations include estimates of the uncertainty due to incomplete knowledge of N<sup>3</sup>LO terms, namely, both the incomplete knowledge of splitting functions, and the missing N<sup>3</sup>LO hard cross-sections, as well as that related to missing perturbative corrections at N<sup>4</sup>LO and beyond. In Ref. [3] (MSHT) the uncertainty estimation is done by means of nuisance parameters, while in Ref. [4] (NNPDF) it is done through a theory covariance matrix. As is well known, (see e.g. Refs. [38, 39]) the nuisance parameter and theory covariance matrix approaches are completely equivalent for Gaussian uncertainties, provided only the eigenvectors and eigenvalues of the covariance matrix coincide with the nuisance parameters and their uncertainties.

The approaches of Refs. [3, 4] consequently only differ in the way the covariance matrix, or the corresponding nuisance parameters, are estimated. In Ref. [3] this is done based on a judicious estimate of the form of missing terms, which also incorporates effects of varying the parametrization of the splitting functions. In Ref. [4], instead, the contributions to the covariance matrix due to incomplete knowledge of splitting functions are estimated differently from all those due to missing higher order terms (missing N<sup>4</sup>LO splitting functions, missing N<sup>4</sup>LO massless DIS coefficient function, and missing N<sup>3</sup>LO hard cross sections for all other processes). Namely, variation of the parametrization of splitting functions (as in Ref. [3]) is used for the estimate of their incomplete knowledge, while renormalization and factorization scale variation is used for missing higher order perturbative corrections.

Both Refs. [3, 4] included all the information that was available at the time of their publication, and consequently, because Ref. [3] was published earlier, it included less information on N<sup>3</sup>LO evolution, and specifically it did not yet include the more recent information on Mellin moments from Refs. [11, 14–16, 40], and the exact knowledge of the heavy quark transition matrix elements, both of which are instead included in Ref. [4] (with the only exception of the heavy quark terms of Ref. [30]) as they had become available meanwhile. Neither determination includes the higher moments of  $P_{gq}$  [17] and  $P_{gg}$  [18, 19]. Some uncertainties in Ref. [3] are accordingly larger, but with the information now available it is possible to check that uncertainties in Refs. [3, 4] were estimated accurately.

Specifically, the uncertainty on splitting functions with Mellin moments up to  $N = 20$  for all matrix

elements but  $P_{gg}$  was assessed in both Refs. [4, 16] with very similar results, and shown in Ref. [4] to be smaller than the uncertainty due to the missing  $N^4LO$  corrections estimated by scale variation. This assessment was extended to  $P_{gg}$  recently in Ref. [19]. The only other uncertainty on perturbative evolution present in Ref. [4] are the contributions, computed in Ref. [30], to transition matrix elements, which however were found in Ref. [30] to agree perfectly within the uncertainty band with the previous approximation [20] adopted in Ref. [4]. Based on this, it can be safely concluded that, as mentioned,  $N^3LO$  perturbative evolution is fully known for all practical purposes. Furthermore, the splitting functions of Refs. [3, 4] agree within uncertainties, with the exception of the  $P_{gq}$  splitting function, that differs at approximately the two-sigma level, see also the benchmarking comparison of [41, 42]. Note, however, that as far as PDF evolution is concerned  $P_{gg}$  is much more important than  $P_{gq}$ , and the effects at small- $x$  are to a large extent anti-correlated. Updated knowledge of the splitting functions effectively removes this one source of moderate discrepancy.

A preliminary analysis of the effect of including these additional Mellin moments, and hence improved splitting functions, which have been determined since the original MSHT publication was presented in [43], and observed a small increase in the gluon near  $x = 0.01$ , though still within the original MSHT uncertainties. While this is significantly washed out in parton luminosities, it does further improve the agreement between the two PDF sets. Furthermore, updated PDF sets obtained using a parametrization of the  $N^3LO$  splitting function constructed in [19] that includes the full information on Mellin moments (and most recently by MSHT, also the complete heavy quark transition matrix elements already used by NNPDF) now available have been presented in preliminary form both by MSHT [44, 45] and NNPDF [46]. These preliminary results allow for a comparison in which all the currently available information on perturbative evolution is consistently used by the two groups. Based on these results, it can be concluded that, whereas the use of a common parametrization of splitting functions and transition matrix elements reduces somewhat the differences between the MSHT and NNPDF a $N^3LO$  PDF sets, results change by a small amount. We shall come back to this point in Sect. 4 below.

Estimates of the impact of the use of a $N^3LO$  PDFs in the computation of the Higgs total production cross-section in both Refs. [3, 4] suggest that using NNLO PDFs, instead of a $N^3LO$  PDFs, with the  $N^3LO$  matrix element for Higgs production in gluon fusion and vector boson fusion leads to an error that is comparable to, or even larger than the PDF uncertainty on the  $N^3LO$  result. Also, this error is found [4] to be rather larger than the estimate of its size based on the corresponding shift at one less perturbative order [47, 48]. This suggests that using NNLO PDFs in the  $N^3LO$  computation spoils the accuracy of the  $N^3LO$  result, in a way that, moreover, may not be reflected in a corresponding increase in uncertainty, if the latter is estimated in this way.

Given the availability of two different a $N^3LO$  PDF sets, accurate  $N^3LO$  phenomenology requires therefore a comparison of the impact of the use of either of these PDF sets, and a prescription for their combination. It is the purpose of this brief note to provide a first assessment and suggest a possible prescription, having specifically in view Higgs production in gluon fusion, but presenting results also for other Higgs production modes. We will first compare the a $N^3LO$  PDFs of Refs. [3, 4], both without and with QED corrections, to each other, then assess for each of them the impact of a $N^3LO$  corrections on parton luminosities, and finally construct a combination of these PDFs based on the PDF4LHC combination methodology [49]. We will finally discuss results for the cross-section for Higgs production in gluon fusion and other channels based on individual and combined a $N^3LO$  PDF sets.

## 2 Comparison of a $N^3LO$ PDFs

We will compare NNPDF4.0 and MSHT PDF sets both with and without QED effects. The QED sets include a photon PDF that mixes with the quark and gluon PDFs upon combined QED $\times$ QCD evolution, and mostly differ from the pure QCD set due to slight depletion of the gluon PDF due to the momentum fraction carried by the photon. They are consequently important when assessing the behavior of the gluon PDF.

When comparing MSHT and NNPDF PDF sets, care must be taken to compare sets that include the same uncertainties. Specifically, all NNPDF4.0 PDF sets are now delivered in two different versions, one in which the PDF uncertainty includes the uncertainty due to missing higher-order corrections on the theory predictions used for PDF determination (MHOU, henceforth), and the other in which it does not. Hence uncertainties due to missing  $N^4LO$  corrections are only included by NNPDF in the a $N^3LO$  MHOU sets,

though both NNPDF and MSHT aN<sup>3</sup>LO sets include uncertainties due to missing N<sup>3</sup>LO corrections to hadronic processes and massive DIS. Note that the NLO and NNLO sets with MHOUs were not included at the time of first release of NNPDF4.0 [2], and only released at a later stage [50]. On the other hand, in the MSHT approach all uncertainties, including all MHOUs, are included at N<sup>3</sup>LO, while MHOUs are not included at NNLO (as they were not in the original NNLO NNPDF4.0 PDFs of Ref. [2]). The pertinent comparison of the MSHT20 sets is therefore at N<sup>3</sup>LO with the NNPDF4.0 sets with MHOUs included, while at NNLO with the NNPDF4.0 sets without MHOUs. Note that in Ref. [4] the MSHT20 aN<sup>3</sup>LO PDFs were instead compared to the NNPDF4.0 set without MHOUs. Henceforth we will here tacitly assume that for NNPDF4.0 NNLO refers to the non-MHOUs while aN<sup>3</sup>LO refers to the MHOUs sets.

When comparing the aN<sup>3</sup>LO PDF sets, it should of course be borne in mind that the MSHT20 and NNPDF4.0 sets already differ at NNLO due to differences in dataset and methodology. On top of the difference in basic underlying methodology, namely generalized polynomial parametrization and Hessian uncertainties for MSHT, neural network parametrization and Monte Carlo uncertainties for NNPDF, several details of the theoretical approach also differ. Specifically, there are several differences in the treatment of heavy quarks: the values of heavy quark masses are somewhat different; the charm PDF is fitted to the data in NNPDF4.0, while in MSHT20 it is determined by perturbative matching conditions; and for DIS the massive and massless heavy quark schemes are matched using the Thorne-Roberts scheme by MSHT and the FONLL scheme by NNPDF. A detailed comparison of the NNLO MSHT20 and NNPDF4.0 PDF sets was performed in Ref. [2], see in particular Fig. 21 and Fig. 60 of that reference. Several of the differences seen in the comparison of Ref. [2] are also seen when comparing MSHT20 to the previous NNPDF3.1 PDF set, and indeed many of the methodological differences (in particular those related to the treatment of heavy quarks) are the same. This is relevant because MSHT20 and NNPDF3.1 were included in a detailed benchmarking presented in Ref. [51, 52], along with the CT18 PDF set. In this work, dedicated PDF sets from the three groups were produced by adopting common assumptions and settings (specifically for the treatment of heavy quarks), instead of the inconsistent settings used in the original fits, as well as a relatively similar global dataset. These PDF sets were called “reduced” in Ref. [51] (though not based on a reduced dataset). These dedicated sets turned out to be in quite good agreement with each other within uncertainties, thereby showing that the differences between the original sets were partly due to these inconsistent settings.

These more consistent sets were then used to produce the PDF4LHC21 combination [51]. The combination that we will discuss here is instead based on the publicly available aN<sup>3</sup>LO PDF sets, thereby leading to a more conservative uncertainty estimate that encompasses the differences between the PDF sets entering the combination, as we shall explain below. To understand the features of this combination we therefore start with a comparison of the published MSHT20 and NNPDF4.0 aN<sup>3</sup>LO sets, along with the NNLO sets, to see how much of the differences seen at aN<sup>3</sup>LO reflect those already present at NNLO, whose origin was largely understood in Refs. [51, 52].

The comparison of the aN<sup>3</sup>LO sets is presented in Figs. 1-2 (left), together with the comparison of the corresponding NNLO sets (right). The aN<sup>3</sup>LO sets including QED corrections are compared in Fig. 3. All PDFs are shown at  $Q = 100$  GeV, normalized to the NNPDF4.0 central value. All error bands are one sigma uncertainties. The dominant differences between the aN<sup>3</sup>LO PDF sets are essentially the same as at NNLO, with the largest difference observed for the charm PDF, which, as mentioned, is independently parametrized in NNPDF4.0, but not in MSHT20, where it is determined by perturbative matching conditions. Indeed, it is clear from Figs. 1-2 that most differences between MSHT and NNPDF change very little when moving from NNLO to aN<sup>3</sup>LO. An exception is the gluon PDF, which differs more between NNPDF and MSHT at aN<sup>3</sup>LO. Specifically, while reasonably compatible for  $x \lesssim 0.07$  at NNLO, the MSHT and NNPDF gluons disagree at aN<sup>3</sup>LO, with the MSHT20 result suppressed in comparison to NNPDF4.0 by 3-4% in the region  $10^{-3} \lesssim x \lesssim 10^{-1}$ , with a PDF uncertainty of 1-2%.

This suppression can, to some extent, be traced to the difference in the behavior of  $P_{gq}$  mentioned in the introduction. The  $P_{gq}$  splitting function contains more unknown small- $x$  divergent terms than the other splitting functions, and hence has more potential uncertainty at small  $x$ , especially if a color-charge relationship that would relate these unknown terms to known contributions to  $P_{gq}$  is not assumed to be approximately true for subleading terms (and indeed it is assumed by NNPDF but not by MSHT). Hence, with the smaller moment information and weaker constraints used by MSHT [3], deviations are possible but have been largely eliminated with the improved information now available.

In practice, the differences between the two aN<sup>3</sup>LO PDF sets are at most at the two sigma level. Furthermore, a recent MSHT preliminary study shows that updating the splitting function with the additional moments now known [14–16] results in a  $\sim 1.5\%$  increase in the gluon at  $x \sim 0.01$  [43], though it does still

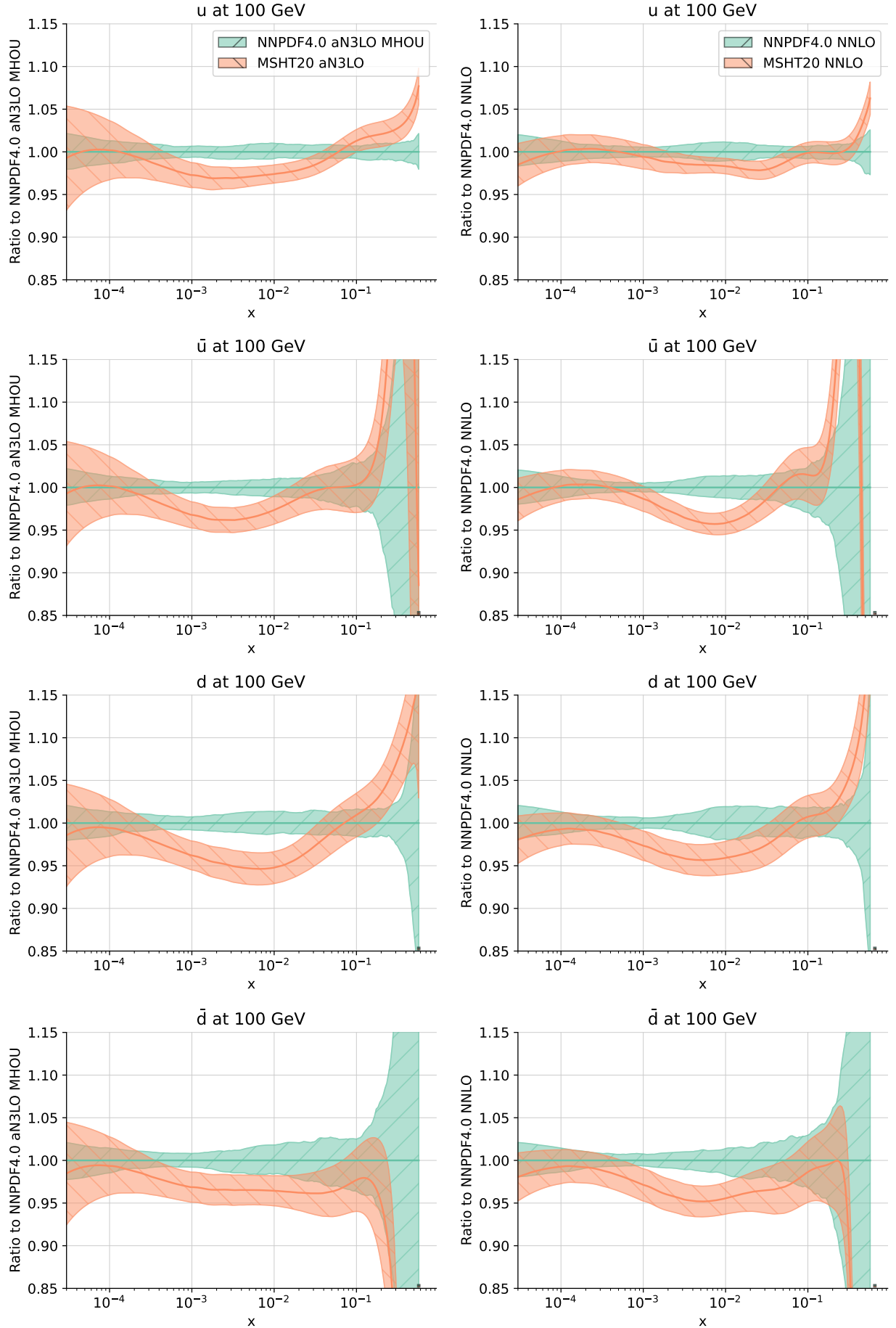


**Figure 1.** The NNPDF4.0 [4] and MSHT20 [3]  $aN^3LO$  (left) and  $NNLO$  (right) PDFs, for the  $u$  and  $d$  sector at  $Q = 100$  GeV, shown as a ratio to NNPDF4.0. All uncertainties shown are one sigma.

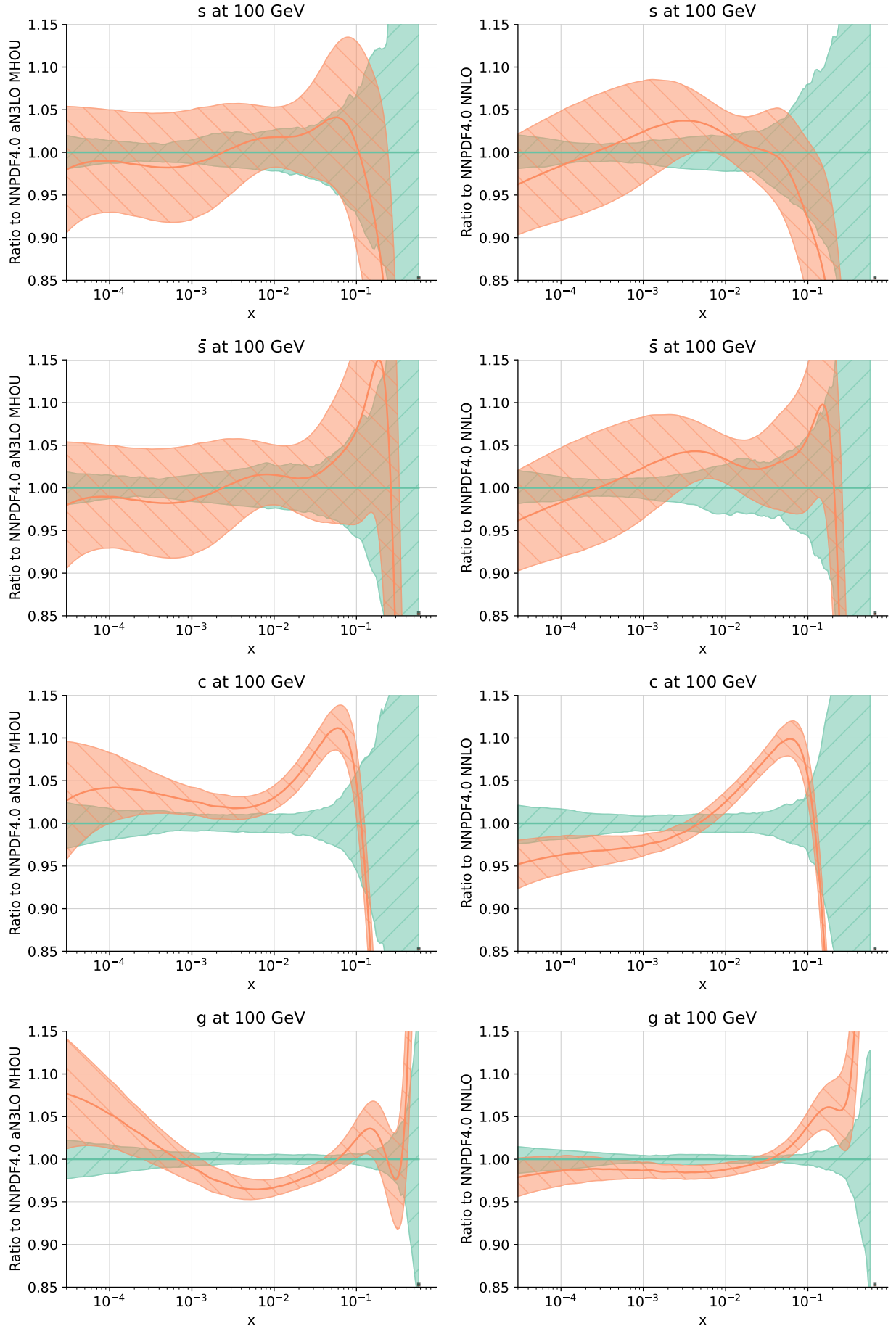


**Figure 2.** As in Fig. 1 but for the  $s, \bar{s}, c, g$  PDFs.

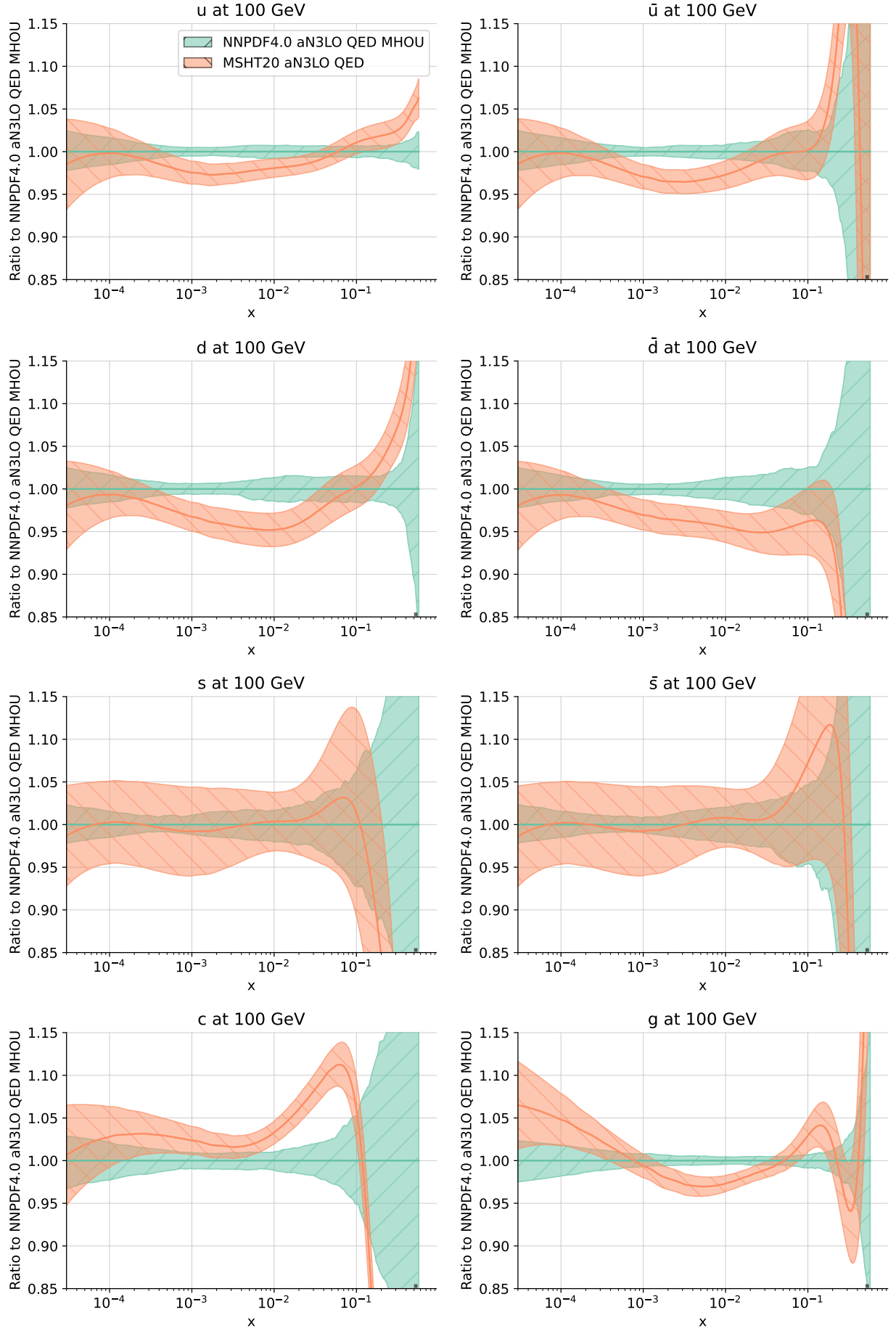


**Figure 3.** The NNPDF4.0 [6] and MSHT20 [5] aN<sup>3</sup>LO+QED PDFs at  $Q = 100$  GeV, shown as a ratio to NNPDF4.0. All uncertainties shown are one sigma.

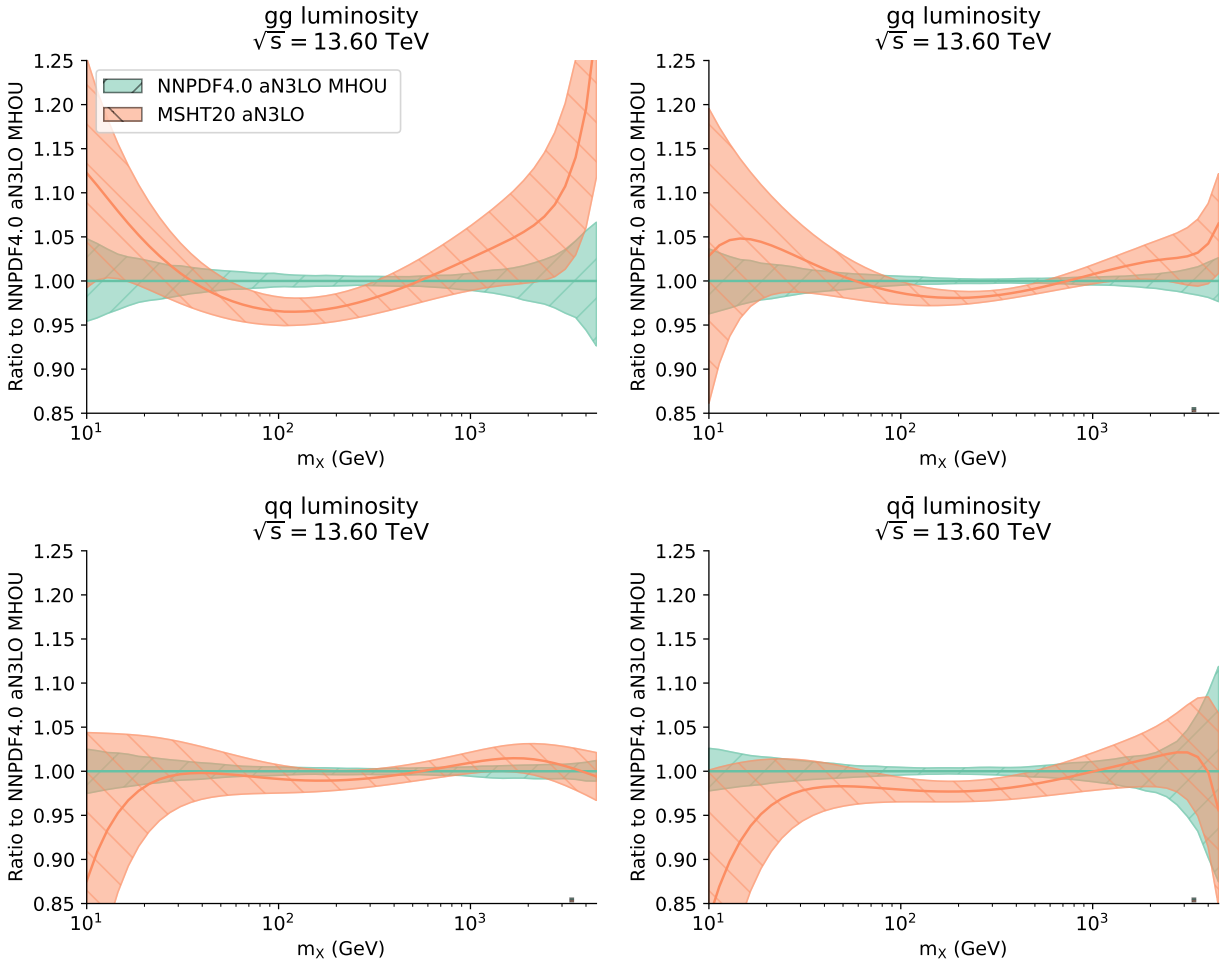


**Figure 4.** The same comparison as in Figs. 1–2 (right) but for the corresponding parton luminosities.

remain within the uncertainty band of the original MSHT determination, thereby further reducing differences. Hence, updates in  $P_{gq}$  do improve the comparison, but do not remove the difference in the gluon. Recall however that, as mentioned in Sect. 1, the very recent additional moments now known for  $P_{gq}$  [17] and  $P_{gg}$  [18, 19] are not included in either the MSHT or NNPDF sets discussed here. Finally, the inclusion of the photon PDF also has a moderate impact on the other PDFs, mostly limited to a suppression of the gluon PDF due to the 1% shift in momentum fraction from the gluon to the photon, as well as some reduction in the  $u, \bar{u}$  PDFs at high  $x$ , due to  $q \rightarrow q\gamma$  splitting.

The MSHT and NNPDF aN<sup>3</sup>LO parton luminosities are compared in Figs. 4–5, respectively without and with QED effects, while, in order to appreciate better the impact of N<sup>3</sup>LO corrections, the aN<sup>3</sup>LO luminosities (without QED) are compared for each set to the respective NNLO luminosities in Fig. 6, normalized to the aN<sup>3</sup>LO result. The pattern of differences reproduces that seen at the level of PDFs, with a suppression of the MSHT gluon-gluon, quark-antiquark, and gluon-quark luminosities in comparison to NNPDF in the  $M_X \sim 100$  GeV region, while the quark-quark luminosity in the two sets is very similar. The suppression can be traced to the behavior of the light quark and gluon PDFs seen in Figs. 1–2 (right). Interestingly, the difference in gluon-gluon luminosity is slightly reduced for the QED PDF sets compared to the pure QCD sets.

The qualitative impact of the aN<sup>3</sup>LO corrections on either set for  $M_X \gtrsim 30$  GeV is similar (and almost identical for the quark-quark luminosity), but with a stronger aN<sup>3</sup>LO suppression of gluon luminosities for MSHT20. In particular the gluon-gluon luminosity is suppressed for  $10^2 \lesssim m_X \lesssim 10^3$  GeV by about 3% in NNPDF4.0 and up to 6% in MSHT20 and the gluon-quark luminosity is suppressed in the same region by about 1% in NNPDF4.0 and 3% in MSHT20. Note that the impact on this comparison of the aforementioned update studied in Ref. [43] of the splitting functions in MSHT is very small due to the integration over rapidity washing out small differences in the gluon.

These comparisons show that the differences between NNLO and aN<sup>3</sup>LO for each set are generally larger than the differences between the two aN<sup>3</sup>LO sets, or indeed the two NNLO sets, especially in the

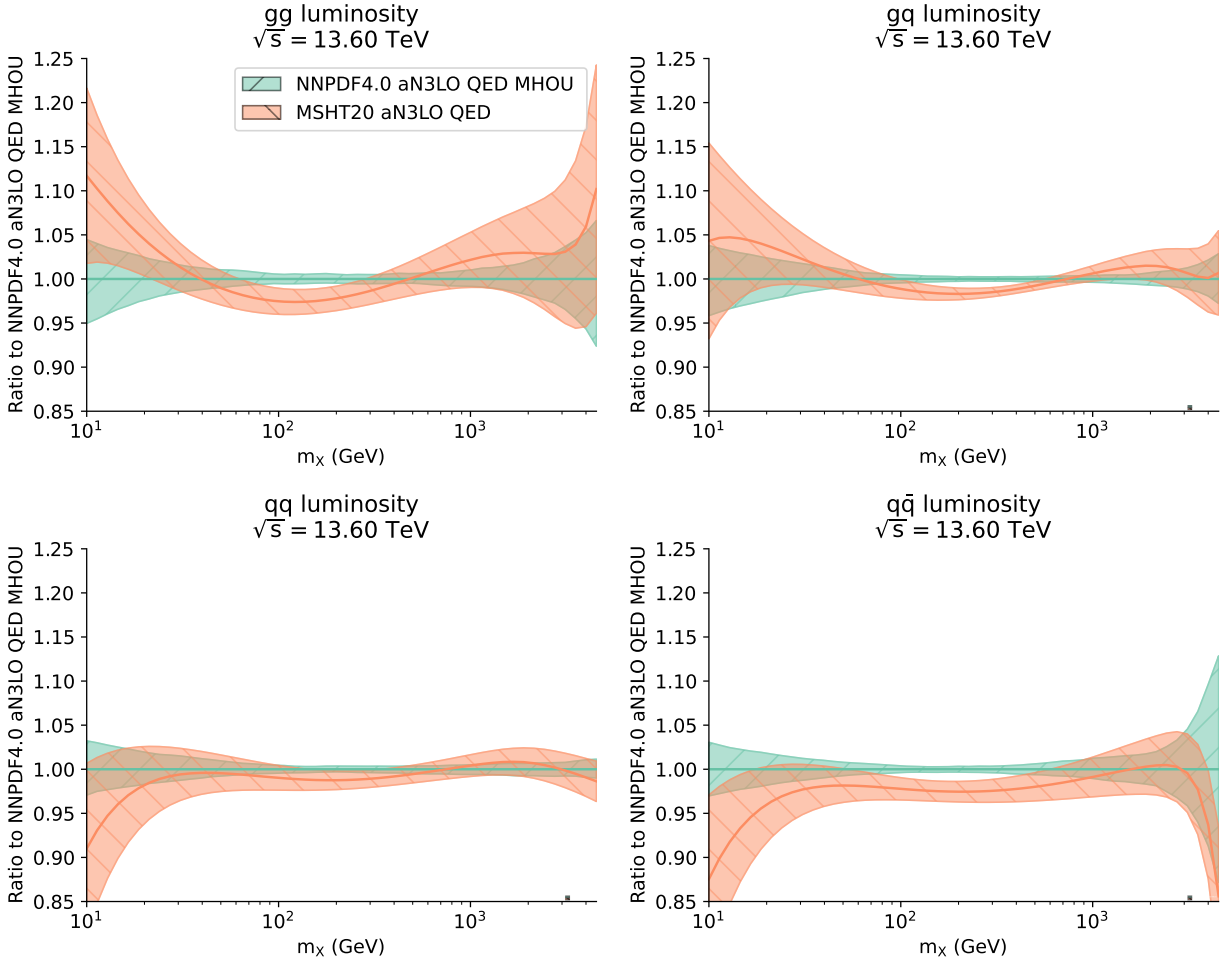


**Figure 5.** The same comparison as in Fig. 4 but including QED corrections.

case of MSHT. Furthermore, the differences between NNLO and aN<sup>3</sup>LO PDFs are often comparable and sometimes (specifically for the gluon-gluon luminosity) larger than the respective PDF uncertainties. These two observations taken together suggest that the use of aN<sup>3</sup>LO PDFs is mandatory for accurate N<sup>3</sup>LO phenomenology, because using NNLO PDFs with the aN<sup>3</sup>LO matrix element leads to an error that may be larger than the PDF uncertainty, especially in the Higgs gluon and vector boson fusion channels, that are respectively mostly sensitive to the gluon-gluon and quark-quark luminosities. Therefore, even though the MSHT and NNPDF aN<sup>3</sup>LO PDF sets do not always agree within uncertainties, their combination will lead to results that are more accurate than the use of NNLO PDFs. These considerations motivate the construction of a combined aN3LO PDF set.

### 3 Combination of aN<sup>3</sup>LO PDFs

Based on the PDF comparisons presented in Sect. 2, phenomenological predictions for hadronic processes at N<sup>3</sup>LO could be obtained by simply using the two available aN<sup>3</sup>LO PDF sets and combining results as a weighted average. However, given that the two sets do not always agree within uncertainties, a more conservative way of estimating the uncertainty on the final result is advisable, such as the so-called PDG prescription and variations thereof [53], see also Sect. 12.5 of Ref. [54].

An effective way of arriving at a conservative uncertainty estimate in our case is to produce unweighted Monte Carlo combined PDF sets [49, 55]. This is done by first turning all the PDF sets to be combined into a set of Monte Carlo replicas, which for Hessian sets can be done using the methodology of Ref. [56], and then merging an equal number of replicas from each set into a single replica set. The merged set then corresponds to a probability distribution that is the equally likely combination of the probability distribution of the input sets, and thus will lead to uncertainties that encompass those of the sets that are being combined. This way if combining uncertainties leads to results that are more conservative than those that would be obtained by performing a weighted average, or possibly including correlations from the underlying data; however,

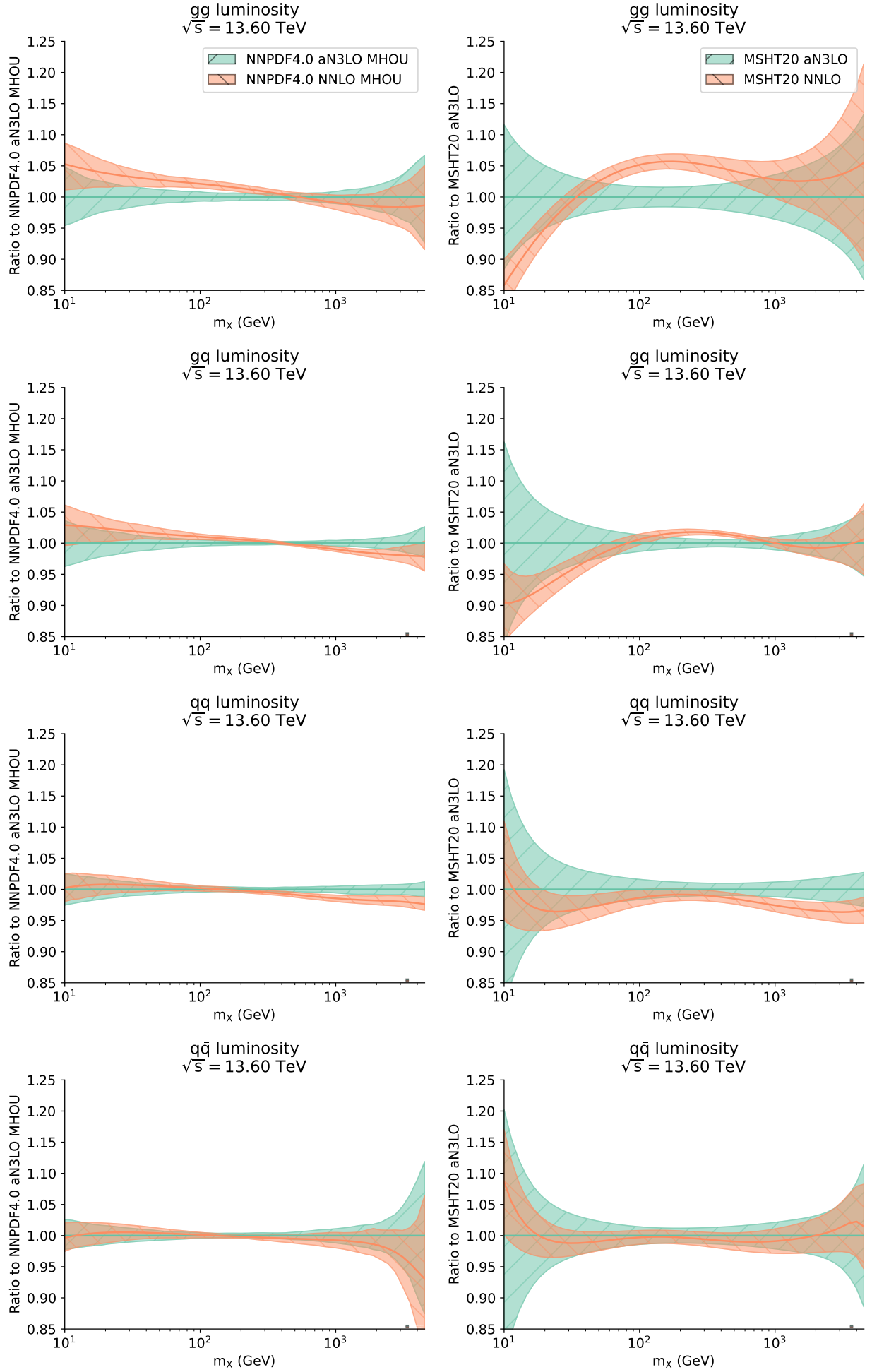


**Figure 6.** Comparison of NNLO and aN<sup>3</sup>LO parton luminosities for NNPDF4.0 [2,4] (left) and MSHT20 [1,3] (right), normalized to the aN<sup>3</sup>LO result.

correlations cannot [57] be reliably taken into account, and differences due to different but equally plausible underlying methodological assumptions are thereby correctly accounted for.

We have produced this combination by merging 100 Monte Carlo replicas produced using the method of Ref. [56] from the default Hessian aN<sup>3</sup>LO set of Ref. [3] after symmetrization of the Hessian uncertainties, with 100 replicas from the MHOU set of Ref. [50]. In order to improve numerical stability of results, for the NNPDF4.0 PDFs the  $(x, Q^2)$  interpolation LHAPDF grid has been recast to match the MSHT20 grid. We have then repeated the procedure for the QED variants presented in Refs. [5, 6]. We will henceforth denote these combined PDF sets as MSHT20xNNPDF40\_an3LO; the corresponding LHAPDF grid files are MSHT20xNNPDF40\_an3lo and MSHT20xNNPDF40\_an3lo\_qed. We have also produced combined pure QCD and QCD $\otimes$ QED NNLO sets obtained using the same procedure, but now starting from the NNPDF4.0 and MSHT NNLO PDF sets. The sole purpose of these sets is to provide a baseline to the corresponding aN<sup>3</sup>LO sets, in order to assess the effect of N<sup>3</sup>LO corrections with everything else unchanged. In particular, they should not be viewed as a substitute for the PDF4LHC21 NNLO combined sets. These sets are denoted as MSHT20xNNPDF40\_NNLO, and the corresponding LHAPDF grid files MSHT20xNNPDF40\_nn1o and MSHT20xNNPDF40\_nn1o\_qed. Note that, as discussed in Sect. 2, the aN<sup>3</sup>LO sets do include while the NNLO sets do not include uncertainties due to MHO in the theory predictions used for PDF determination.

It should always be kept in mind that, as already mentioned, unlike the PDF4LHC21 combined PDFs [51], these aN<sup>3</sup>LO and NNLO MSHT20xNNPDF40 PDFs are an unmodified combination of the two input sets, which are based on somewhat different theoretical and methodological assumptions. They should be viewed as a means to obtain accurate but conservative N<sup>3</sup>LO predictions for LHC processes, not as an optimized PDF combined set. For example, due to the aforementioned different treatment of heavy quarks, the combined PDFs are only reliable for scales well above the heavy quark thresholds, and should not be used in regions where heavy quark mass effects are relevant, such as Higgs production via bottom quark fusion. However, we will show below that for scales  $M_X \gtrsim 50$  GeV the effects of these different treatments of quark masses are in general smaller than the differences between NNLO vs. aN<sup>3</sup>LO PDFs.

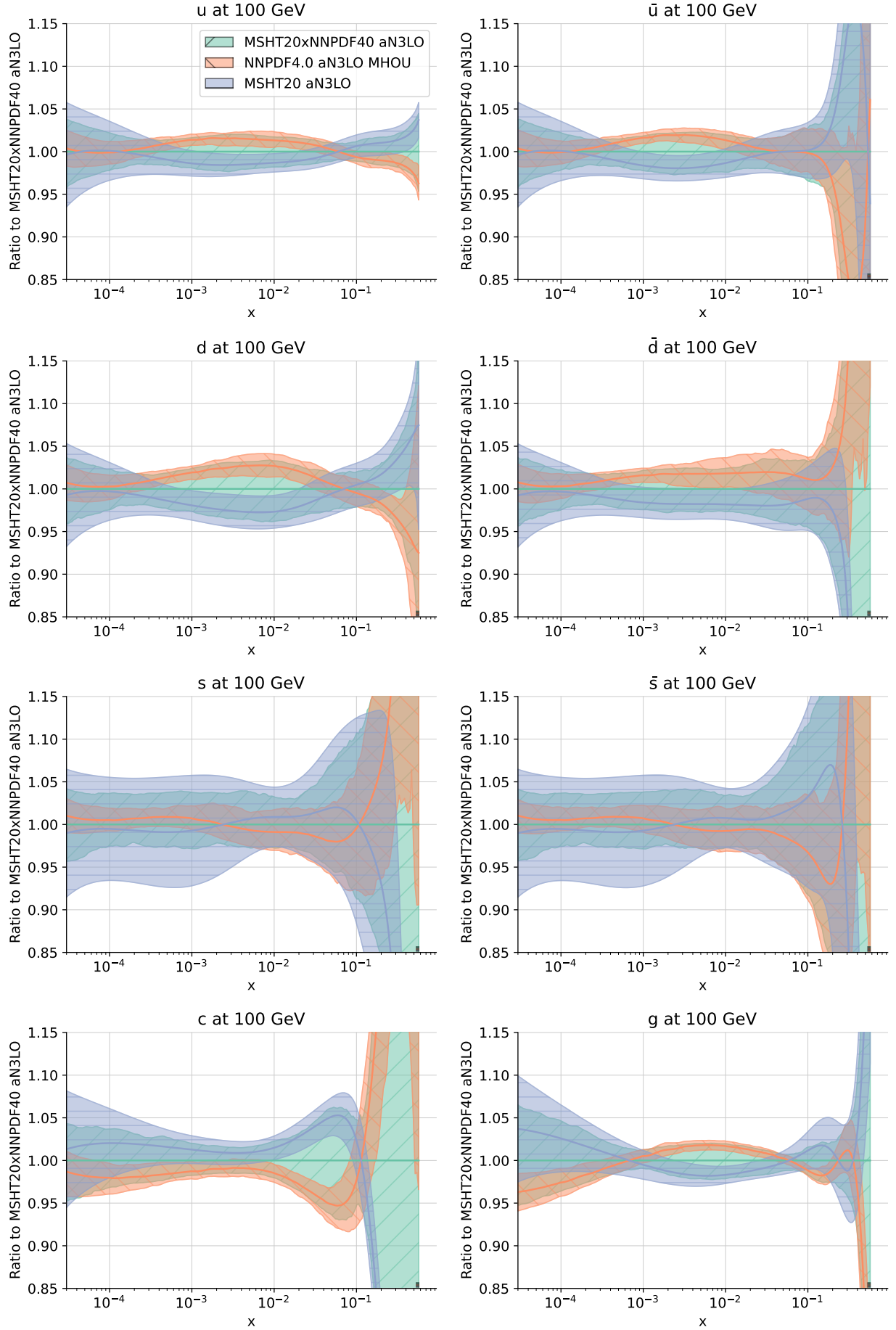
The combined aN<sup>3</sup>LO PDFs are displayed at  $Q = 100$  GeV in Figs. 7–8, respectively without and with QED effects, together with the two sets that are being merged, shown as a ratio to the central value of the combined set. The central value of the combined set is, by construction, the unweighted average of the two starting sets, and the uncertainty is seen to encompass that of the two sets that enter the combination.

In order to assess the impact of the N<sup>3</sup>LO corrections, in Fig. 9 we compare luminosities for the LHC  $\sqrt{s} = 13.6$  TeV at NNLO and aN<sup>3</sup>LO, in the latter case both without and then with QED corrections, shown as a ratio to the NNLO result, computed using the PDF4LHC21 combined NNLO PDF set [51]. For reference, the NNLO sets are compared to each other in Fig. 10, where we show the two different combinations, PDF4LHC21 and MSHT20xNNPDF40\_NNLO, the latter both without and with QED corrections. It is clear that for the gluon-gluon and quark-quark luminosities at all scales  $M_X \gtrsim 100$  GeV the impact of the aN<sup>3</sup>LO corrections is quite significant and in the gluon-gluon channel well outside the NNLO uncertainty band. On the other hand, the difference between the two NNLO combinations is significantly smaller, with each of them well within the uncertainty band of the other, thereby showing that the significance of the aN<sup>3</sup>LO does not depend on the NNLO baseline that one compares it to. For the gluon-gluon luminosity the impact of QED corrections is also significant, both at NNLO and aN<sup>3</sup>LO.

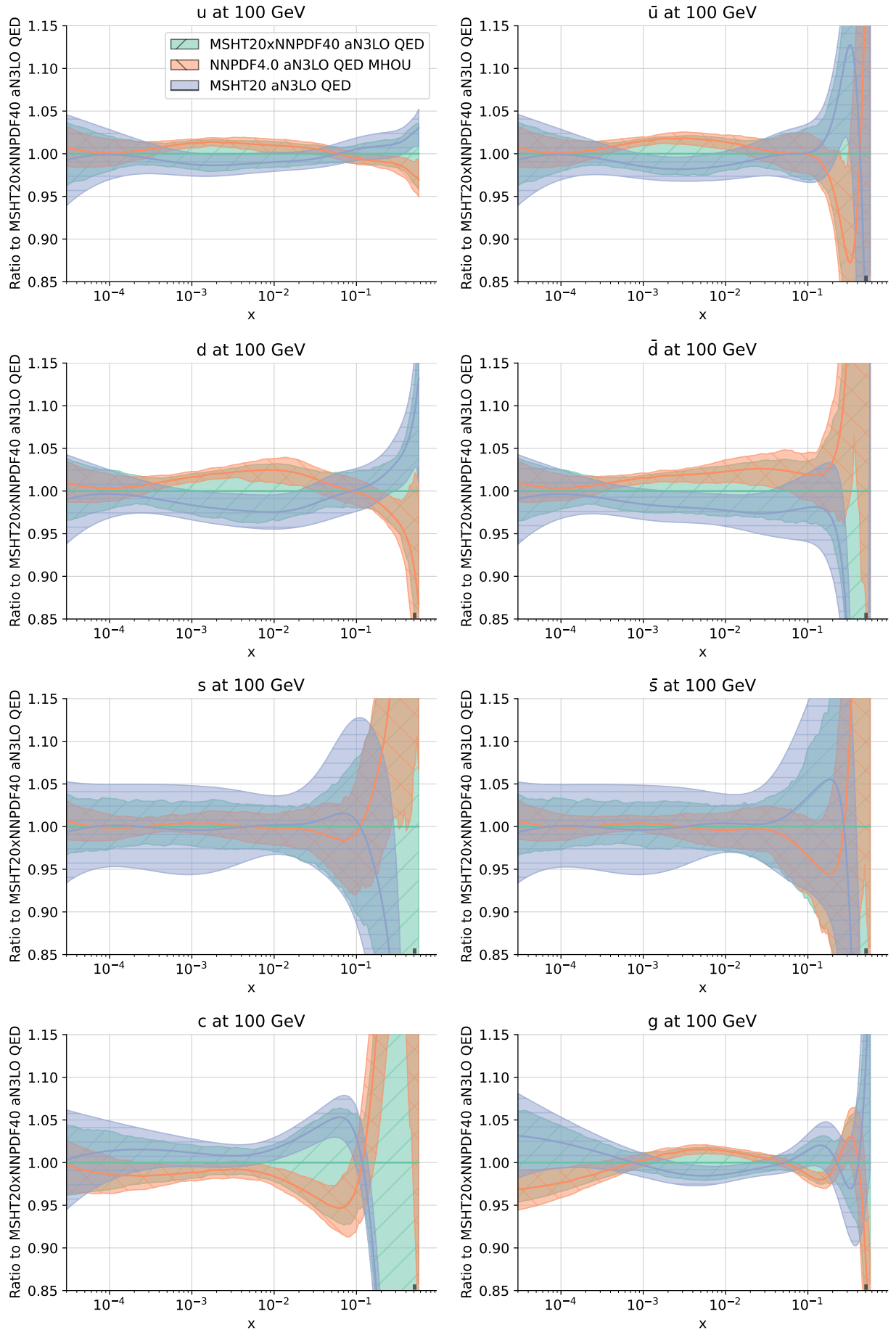
It is interesting to observe that for the gluon-gluon luminosity in the range  $30 \lesssim M_X \lesssim 300$  GeV the difference between aN<sup>3</sup>LO and NNLO is significantly larger than the difference between NNLO and NLO, with the effect peaking around  $M_X \sim 100$  GeV (see Fig. 24 of Ref. [4]), though somewhat reduced upon the inclusion of MHOUs. This can be understood as the consequence of the fact that at N<sup>3</sup>LO there is a leading small  $x$  logarithmic contribution to  $P_{gg}$  and  $P_{gq}$ , which instead accidentally vanishes both at NLO and NNLO. This results in N<sup>3</sup>LO corrections leading to sizable contribution to gluon evolution even at intermediate  $x$ : indeed, both splitting functions at N<sup>3</sup>LO are qualitatively similar to the form that one obtains when including into the splitting function full small- $x$  resummation [4]. Furthermore, the effect of N<sup>3</sup>LO corrections on splitting functions, heavy flavour contributions, and light quark coefficient functions all conspire to push the gluon in the same direction for all  $x \lesssim 0.1$  (see Fig. 44 of Ref. [3]).

## 4 Implications for Higgs production

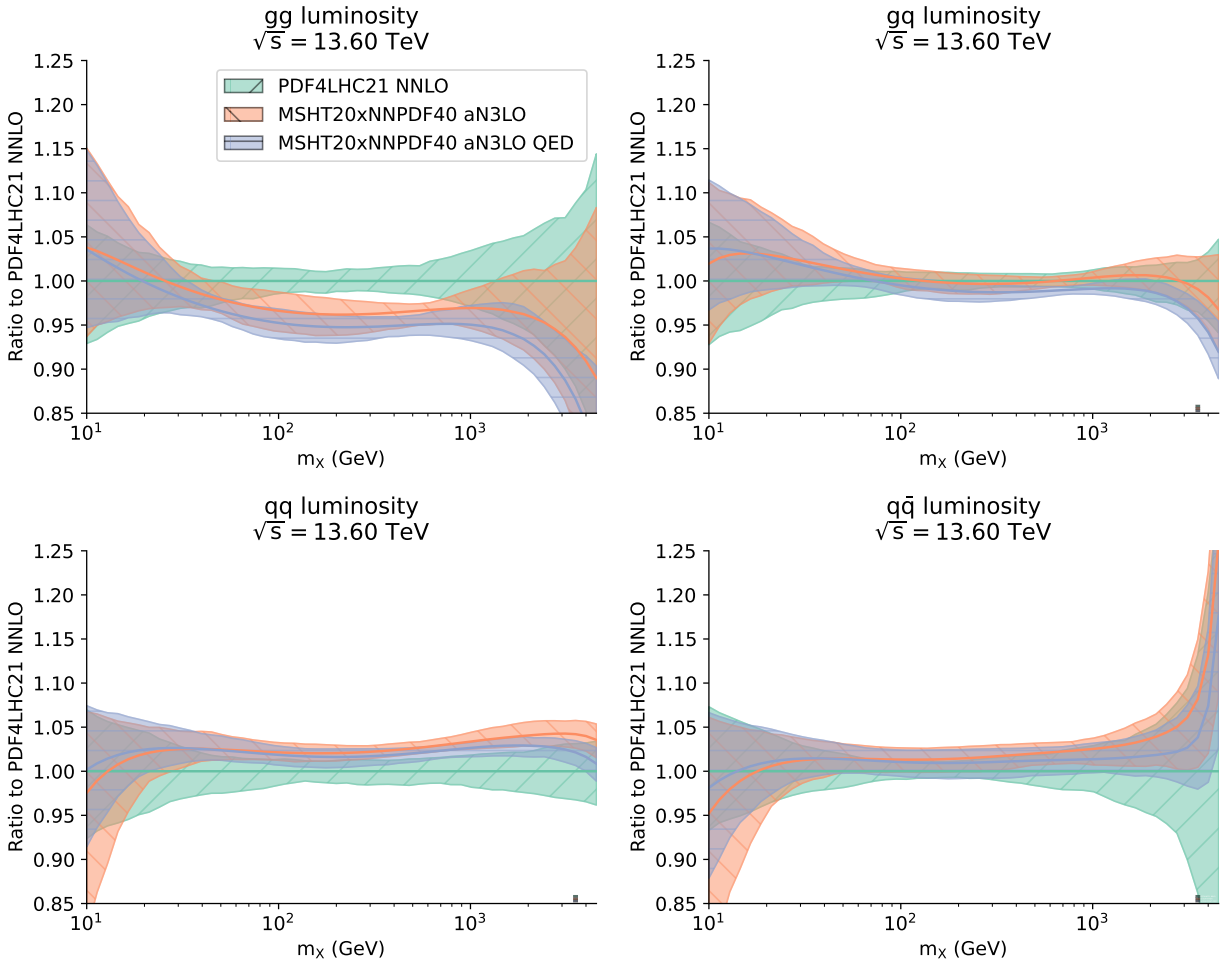
We now present predictions for Higgs production at the LHC in gluon fusion, in vector boson fusion (VBF), and in association with a weak gauge boson ( $hV$ ). Results are collected in Tables 1–2 and displayed in



**Figure 7.** The combined MSHT20xNNPDF40\_aN3LO PDFs, compared to the NNPDF and MSHT aN<sup>3</sup>LO PDFs that enter the combination [3, 4], shown as a ratio to MSHT20xNNPDF40\_aN3LO.



**Figure 8.** Same as Fig. 7, but for the QED PDF sets.



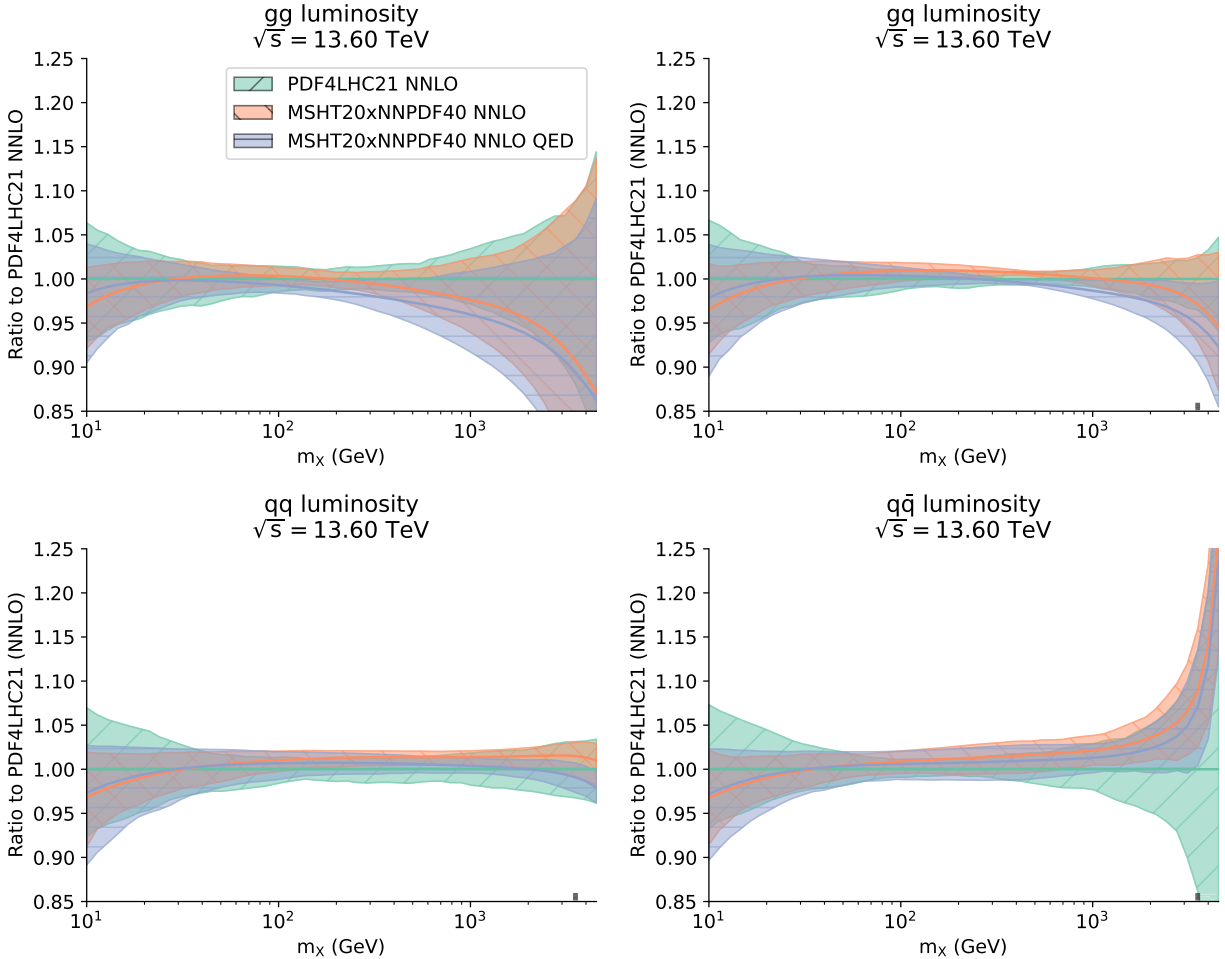
**Figure 9.** Parton luminosities for the LHC  $\sqrt{s} = 13.6$  TeV computed from the MSHT20xNNPDF40\_aN3LO pure QCD and QCD+QED sets, compared to the NNLO PDF4LHC21 result [51], and shown a ratio to the latter.

Fig. 11. All results shown are computed for the LHC with  $\sqrt{s} = 13.6$  TeV using  $N^3LO$  matrix elements, and only differ in the input PDF set. No QED or electroweak corrections are included in the matrix element, and in particular photon-initiated processes are not included. The impact of these on the processes considered here is assessed e.g. in Ref. [58], it is negligible for gluon fusion, of order of a percent for VBF and a few percent for associate production, and it is similar for all PDF sets considered here as the photon PDF in the NNPDF4.0 and MSHT20 sets is quite similar, so it does not affect the comparisons presented here.

The cross-sections are computed using the `ggHiggs` code [59, 60] for gluon fusion, `n3loxs` [47] for associated production, and `proVBFH` [61, 62] for VBF. The central factorization and renormalization scales are set to  $\mu_F = \mu_R = m_H/2$  for Higgs production in gluon fusion,  $\mu_F = \mu_R = Q_V$  (the vector boson virtuality) for VBF, and  $\mu_F = \mu_R = m_{hV}$ , the event-by-event invariant mass of the  $hV$  system, in associated production. In Fig. 11 we do not display the  $hW^-$  cross-sections since they have the same qualitative behavior as the  $hW^+$  cross-sections, as can also be observed from Table 1.

The uncertainties shown in Tables 1-2 and in Fig. 11 are the pure PDF uncertainty (first uncertainty in the table and inner error bar in the figure) as well as the sum in quadrature of the PDF uncertainty and MHO uncertainties on the matrix element, the latter evaluated with the 7 point scale variation prescription (second uncertainty in the table and outer error bar in the figure). For the VBF and  $hV$  production channels the two uncertainties essentially coincide, because scale variations are negligible and the PDF uncertainty dominates, while in the gluon-fusion cross-sections scale errors represent the largest theoretical uncertainty.

Results are shown for the MSHT20 and NNPDF4.0 aN<sup>3</sup>LO sets both with and without QED corrections, and the combined MSHT20xNNPDF40 aN<sup>3</sup>LO sets constructed here, also with and without QED corrections. Results obtained by using perturbatively mismatched NNLO PDFs together with the  $N^3LO$  matrix element are also shown, both for the PDF4LHC21 and MSHT20xNNPDF40 NNLO combined sets. In order to visually assess the error involved in this procedure, in Fig. 11 we also show results as a ratio of the result to that found using mismatched NNLO PDFs, specifically from the MSHT20xNNPDF40\_NNLO combined baseline set.



**Figure 10.** Comparison of NNLO parton luminosities for the LHC with  $\sqrt{s} = 13.6$  TeV: the MSHT20xNNPDF40\_nnlo pure QCD and QCD+QED results are compared to the PDF4LHC21 combination [51].

The percentage error made when using mismatched NNLO PDFs is

$$\Delta_{\text{NNLO}}^{\text{exact}} \equiv \left| \frac{\sigma_{\text{aN}^3\text{LO-PDF}}^{\text{N}^3\text{LO}} - \sigma_{\text{NNLO-PDF}}^{\text{N}^3\text{LO}}}{\sigma_{\text{aN}^3\text{LO-PDF}}^{\text{N}^3\text{LO}}} \right|. \quad (1)$$

An approximate way of estimating this error before knowledge of aN<sup>3</sup>LO PDFs, based on the behavior seen at one less perturbative order, was suggested in Refs. [47, 48] and it is given by

$$\Delta_{\text{NNLO}}^{\text{app}} \equiv \frac{1}{2} \left| \frac{\sigma_{\text{NNLO-PDF}}^{\text{NNLO}} - \sigma_{\text{NLO-PDF}}^{\text{NNLO}}}{\sigma_{\text{NNLO-PDF}}^{\text{NNLO}}} \right|. \quad (2)$$

The values of  $\Delta_{\text{NNLO}}^{\text{exact}}$  and  $\Delta_{\text{NNLO}}^{\text{app}}$  obtained for each process are also included in Tables 1-2, both for NNPDF4.0, MSHT20, and the combined PDF sets constructed here, using in each case PDFs at the required perturbative orders from the same set. For the computation of  $\Delta_{\text{NNLO}}^{\text{app}}$  for the combined set we use as a value for  $\sigma_{\text{NLO-PDF}}^{\text{NNLO}}$  the average of the cross-sections computed using NNPDF4.0 and MSHT20 NLO PDFs.

It is clear that, as already noticed from the comparison of parton luminosities of Figs. 9-10, the effect of using aN<sup>3</sup>LO PDFs is most substantial for gluon fusion and vector boson fusion, which depend on the gluon-gluon and quark-quark luminosity respectively, and is small for associated  $hV$  production, which depends on the quark-antiquark luminosity. It follows that for gluon fusion and VBF using mismatched NNLO PDFs leads to a large error  $\Delta_{\text{NNLO}}^{\text{exact}}$ . Furthermore, the approximate estimate of this error  $\Delta_{\text{NNLO}}^{\text{app}}$  is very unreliable, and specifically for gluon fusion and VBF it underestimates the true  $\Delta_{\text{NNLO}}^{\text{exact}}$  significantly. The fact that for gluon fusion  $\Delta_{\text{NNLO}}^{\text{app}}$  is rather smaller than  $\Delta_{\text{NNLO}}^{\text{exact}}$  means that the difference between using N<sup>3</sup>LO and NNLO PDFs is significantly larger than one may expect comparing the change at the previous order, thus belying expectations [48, 63] that the impact of N<sup>3</sup>LO PDFs would be very small based on the behavior of the previous orders. This is a consequence of the behavior of the gluon luminosity discussed at the end of Sect. 3.

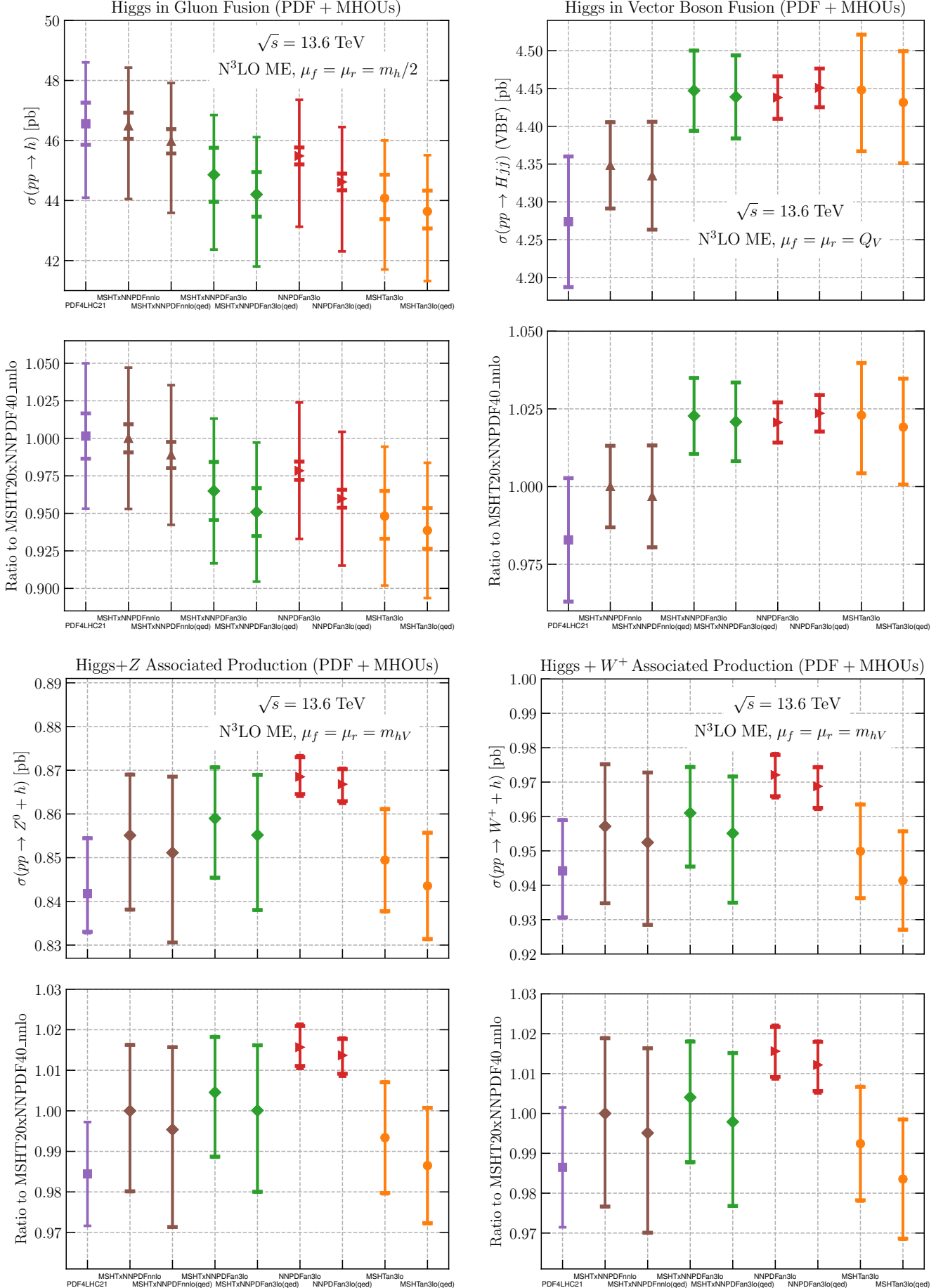


**Figure 11.** The cross-sections of Tables 1-2, shown both in absolute scale (top) or as ratios to the result found using the MSHT20xNNPDF40\_nnlo baseline combination. In all cases,  $N^3LO$  matrix elements are used. The results for  $hW^-$  are qualitatively similar as those for  $hW^+$  and not shown. The inner interval is the pure PDF uncertainty (first uncertainty in Tables 1-2) while the outer interval is the sum in quadrature of the PDF uncertainty and the MHOU uncertainty on the hard cross section (second uncertainty in Tables 1-2).

PDF set	pert. order (PDF)	$\sigma(gg \rightarrow h)$	$\sigma(h \text{ VBF})$
PDF4LHC21_mc	NNLO <sub>QCD</sub>	$46.56^{+1.5\%}_{-1.5\%} {}^{+4.4\%}_{-5.3\%}$	$4.27^{+2.0\%}_{-2.0\%} {}^{+2.0\%}_{-2.0\%}$
MSHT20xNNPDF40_nnlo	NNLO <sub>QCD</sub>	$46.49^{+0.9\%}_{-0.9\%} {}^{+4.2\%}_{-5.3\%}$	$4.35^{+1.3\%}_{-1.3\%} {}^{+1.3\%}_{-1.3\%}$
MSHT20xNNPDF40_nnlo_qed	NNLO <sub>QCD</sub> $\otimes$ NLO <sub>QED</sub>	$45.97^{+0.9\%}_{-0.9\%} {}^{+4.3\%}_{-5.4\%}$	$4.34^{+1.6\%}_{-1.6\%} {}^{+1.6\%}_{-1.6\%}$
MSHT20xNNPDF40_an3lo	aN <sup>3</sup> LO <sub>QCD</sub>	$44.86^{+2.0\%}_{-2.0\%} {}^{+4.4\%}_{-5.6\%}$	$4.45^{+1.2\%}_{-1.2\%} {}^{+1.2\%}_{-1.2\%}$
MSHT20xNNPDF40_an3lo_qed	aN <sup>3</sup> LO <sub>QCD</sub> $\otimes$ NLO <sub>QED</sub>	$44.20^{+1.7\%}_{-1.7\%} {}^{+4.3\%}_{-5.4\%}$	$4.44^{+1.2\%}_{-1.2\%} {}^{+1.2\%}_{-1.2\%}$
NNPDF40_an3lo_as_01180_mhou	aN <sup>3</sup> LO <sub>QCD</sub>	$45.49^{+0.6\%}_{-0.6\%} {}^{+4.1\%}_{-5.2\%}$	$4.44^{+0.6\%}_{-0.6\%} {}^{+0.7\%}_{-0.6\%}$
NNPDF40_an3lo_as_01180_qed_mhou	aN <sup>3</sup> LO <sub>QCD</sub> $\otimes$ NLO <sub>QED</sub>	$44.62^{+0.6\%}_{-0.6\%} {}^{+4.1\%}_{-5.2\%}$	$4.45^{+0.6\%}_{-0.6\%} {}^{+0.6\%}_{-0.6\%}$
MSHT20an3lo_as118	aN <sup>3</sup> LO <sub>QCD</sub>	$44.08^{+1.8\%}_{-1.6\%} {}^{+4.4\%}_{-5.6\%}$	$4.44^{+1.6\%}_{-1.8\%} {}^{+1.7\%}_{-1.8\%}$
MSHT20qed_an3lo	aN <sup>3</sup> LO <sub>QCD</sub> $\otimes$ NLO <sub>QED</sub>	$43.63^{+1.6\%}_{-1.3\%} {}^{+4.3\%}_{-5.3\%}$	$4.43^{+1.5\%}_{-1.8\%} {}^{+1.5\%}_{-1.8\%}$
$\Delta_{\text{NNLO}}^{\text{exact}} (\text{NNPDF4.0})$		2.2%	1.3%
$\Delta_{\text{NNLO}}^{\text{exact}} (\text{MSHT20})$		5.3%	2.3%
$\Delta_{\text{NNLO}}^{\text{exact}} (\text{combination})$		3.3%	2.3%
$\Delta_{\text{NNLO}}^{\text{app}} (\text{NNPDF4.0})$		0.2%	0.2%
$\Delta_{\text{NNLO}}^{\text{app}} (\text{MSHT20})$		1.4%	1.3%
$\Delta_{\text{NNLO}}^{\text{app}} (\text{combination})$		0.9%	0.5%

**Table 1.** The total inclusive cross-section (in pb) for Higgs production in the gluon-fusion and VBF channels at the LHC Run 3 with  $\sqrt{s} = 13.6$  TeV. In all cases, the partonic matrix element is evaluated at N<sup>3</sup>LO accuracy not including QED or electroweak corrections. The central scales are set to be  $\mu_{F,R} = m_H/2$  (gluon fusion) and  $\mu_{F,R} = Q_V$  (VBF). The first uncertainty shown is the pure PDF uncertainty, and the second is the sum in quadrature of the PDF uncertainty and the MHOU on the hard cross-section evaluated with the 7-point prescription. The PDF4LHC21\_mc [51] and MSHT20xNNPDF40\_nnlo PDF sets are at NNLO, while all the other PDF sets [3, 4] are determined at aN<sup>3</sup>LO accuracy. The error  $\Delta_{\text{NNLO}}^{\text{exact}}$ , Eq. (1), that is made when using NNLO PDFs with the aN<sup>3</sup>LO matrix element, and its approximate estimate  $\Delta_{\text{NNLO}}^{\text{app}}$ , Eq. (2), are also provided both separately for NNPDF4.0, MSHT20, and for their combination in the case of the pure QCD fits.

Indeed, for gluon fusion there is a compensation between the hard cross-section and the gluon PDF when both are used at N<sup>3</sup>LO, with the former leading to a significant increase which is then largely eliminated by the reduced gluon distribution in the correctly matched PDFs. For VBF, instead, the use of aN<sup>3</sup>LO PDFs leads to a clear increase of 2.5% compared to using NNLO PDFs in all cases, much larger than the fixed-order uncertainty.

The choice of a specific PDF (either of the individual sets or any of the combinations) entering the calculation has a relatively small effect on VBF, either at NNLO or aN<sup>3</sup>LO. For gluon fusion this choice has a negligible effect at NNLO, while at aN<sup>3</sup>LO, as repeatedly observed, a stronger suppression is found using MSHT20 than NNPDF4.0 PDFs, with the combination providing a value in between and an uncertainty encompassing the different degrees of suppression. Hence in both cases, the error made using NNLO PDFs is larger than the PDF uncertainties, and also larger than the spread of aN<sup>3</sup>LO results. The picture is somewhat different for associate Higgs production. For this process, the impact of using aN<sup>3</sup>LO vs. NNLO PDFs is negligible, so the dominant difference comes from the choice of PDF set, though results found using

PDF set	pert. order (PDF)	$\sigma(hW^+)$	$\sigma(hW^-)$	$\sigma(hZ)$
PDF4LHC21_mc	NNLO <sub>QCD</sub>	$0.944^{+1.6\%}_{-1.4\%} {}^{+1.6\%}_{-1.5\%}$	$0.593^{+1.5\%}_{-1.2\%} {}^{+1.5\%}_{-1.3\%}$	$0.842^{+1.5\%}_{-1.0\%} {}^{+1.5\%}_{-1.1\%}$
MSHT20xNNPDF40_nnlo	NNLO <sub>QCD</sub>	$0.957^{+1.9\%}_{-2.3\%} {}^{+1.9\%}_{-2.4\%}$	$0.601^{+1.5\%}_{-2.2\%} {}^{+1.6\%}_{-2.2\%}$	$0.855^{+1.6\%}_{-2.0\%} {}^{+1.6\%}_{-2.0\%}$
MSHT20xNNPDF40_nnlo_qed	NNLO <sub>QCD</sub> $\otimes$ NLO <sub>QED</sub>	$0.952^{+2.1\%}_{-2.5\%} {}^{+2.1\%}_{-2.5\%}$	$0.598^{+1.8\%}_{-2.5\%} {}^{+1.8\%}_{-2.5\%}$	$0.851^{+2.0\%}_{-2.4\%} {}^{+2.1\%}_{-2.4\%}$
MSHT20xNNPDF40_an3lo	aN <sup>3</sup> LO <sub>QCD</sub>	$0.961^{+1.4\%}_{-1.6\%} {}^{+1.4\%}_{-1.6\%}$	$0.604^{+1.2\%}_{-1.6\%} {}^{+1.2\%}_{-1.6\%}$	$0.859^{+1.4\%}_{-1.6\%} {}^{+1.4\%}_{-1.6\%}$
MSHT20xNNPDF40_an3lo_qed	aN <sup>3</sup> LO <sub>QCD</sub> $\otimes$ NLO <sub>QED</sub>	$0.955^{+1.7\%}_{-2.1\%} {}^{+1.7\%}_{-2.1\%}$	$0.601^{+1.4\%}_{-2.0\%} {}^{+1.4\%}_{-2.0\%}$	$0.855^{+1.6\%}_{-2.0\%} {}^{+1.6\%}_{-2.0\%}$
NNPDF40_an3lo_as_01180_mhou	aN <sup>3</sup> LO <sub>QCD</sub>	$0.972^{+0.6\%}_{-0.6\%} {}^{+0.7\%}_{-0.7\%}$	$0.610^{+0.6\%}_{-0.6\%} {}^{+0.6\%}_{-0.7\%}$	$0.869^{+0.5\%}_{-0.5\%} {}^{+0.6\%}_{-0.5\%}$
NNPDF40_an3lo_as_01180_qed_mhou	aN <sup>3</sup> LO <sub>QCD</sub> $\otimes$ NLO <sub>QED</sub>	$0.969^{+0.6\%}_{-0.6\%} {}^{+0.6\%}_{-0.7\%}$	$0.608^{+0.5\%}_{-0.6\%} {}^{+0.6\%}_{-0.7\%}$	$0.867^{+0.4\%}_{-0.4\%} {}^{+0.4\%}_{-0.5\%}$
MSHT20an3lo_as118	aN <sup>3</sup> LO <sub>QCD</sub>	$0.950^{+1.4\%}_{-1.4\%} {}^{+1.5\%}_{-1.5\%}$	$0.599^{+1.5\%}_{-1.5\%} {}^{+1.5\%}_{-1.5\%}$	$0.849^{+1.4\%}_{-1.4\%} {}^{+1.4\%}_{-1.4\%}$
MSHT20qed_an3lo	aN <sup>3</sup> LO <sub>QCD</sub> $\otimes$ NLO <sub>QED</sub>	$0.941^{+1.5\%}_{-1.5\%} {}^{+1.5\%}_{-1.5\%}$	$0.595^{+1.6\%}_{-1.6\%} {}^{+1.6\%}_{-1.6\%}$	$0.844^{+1.4\%}_{-1.4\%} {}^{+1.5\%}_{-1.5\%}$
$\Delta_{\text{NNLO}}^{\text{exact}} (\text{NNPDF4.0})$		0.5%	0.3%	0.3%
$\Delta_{\text{NNLO}}^{\text{exact}} (\text{MSHT20})$		0.9%	1.0%	0.8%
$\Delta_{\text{NNLO}}^{\text{exact}} (\text{combination})$		0.6%	0.5%	0.5%
$\Delta_{\text{NNLO}}^{\text{app}} (\text{NNPDF4.0})$		0.2%	0.2%	0.1%
$\Delta_{\text{NNLO}}^{\text{app}} (\text{MSHT20})$		0.8%	0.9%	1.1%
$\Delta_{\text{NNLO}}^{\text{app}} (\text{combination})$		0.1%	0.2%	0.3%

**Table 2.** Same as Table 1 for Higgs production in association with vector bosons.

any of the PDF sets or combinations considered here all agree within uncertainties.

Also, we observe that for Higgs production in gluon fusion the effect of QED corrections, again as already seen in luminosities, is also not negligible, though smaller than that of using properly matched PDFs.

It is also interesting to compare results obtained using the MC combination of aN<sup>3</sup>LO PDF sets to those that would be found by performing the textbook weighted average and uncertainty. For gluon fusion the weighted combination (with weights  $1/\delta_{\text{pdf}}^2$ ) gives

$$\sigma_{\text{ggF}}^{\text{comb}} = 45.30 \pm 0.28_{\text{pdf}} \text{ pb} \quad (\text{pure QCD}) \quad (3)$$

$$\sigma_{\text{ggF}}^{\text{comb}} = 44.43 \pm 0.26_{\text{pdf}} \text{ pb} \quad (\text{QCD+QED}). \quad (4)$$

This is to be compared with the result found using the MSHT20xNNPDF40 aN<sup>3</sup>LO sets (both pure QCD and QCD $\otimes$ QED) from Table 1, namely

$$\sigma_{\text{ggF}}^{\text{MSHTxNNPDF}} = 44.86 \pm 0.90_{\text{pdf}} \text{ pb} \quad (\text{pure QCD}) \quad (5)$$

$$\sigma_{\text{ggF}}^{\text{MSHTxNNPDF-qed}} = 44.20 \pm 0.75_{\text{pdf}} \text{ pb} \quad (\text{QCD+QED}). \quad (6)$$

where in both cases we consider only the PDF uncertainty. It is clear that the latter result is significantly more conservative, in that it treats the two existing sets on the same footing and leads to a correspondingly rather larger uncertainty. Eqs. (5)–(6) should be considered our best result for Higgs production in gluon fusion, although we emphasize that the difference between this and the weighted average remains lower than the difference between the predictions based on NNLO and aN<sup>3</sup>LO PDFs.

Finally, as mentioned in the introduction, we have assessed the effect of using the preliminary variants of the aN<sup>3</sup>LO PDF sets presented here, and recently constructed by MSHT [44, 45] and NNPDF [46] using the

parametrization of aN<sup>3</sup>LO splitting functions of Ref. [19], that includes all the perturbative information that is currently available, and also using for both sets the same N<sup>3</sup>LO heavy quark transition matrix element as used by NNPDF4.0. These preliminary variants have been also used in order to produce a variant combined set. Very moderate differences are found: specifically, for NNPDF, the central value of the gluon-fusion cross-section in the aN<sup>3</sup>LO baseline fit of 45.49 pb (see Table 1) becomes 45.25 pb, namely a shift of  $-0.5\%$ , while for MSHT the aN<sup>3</sup>LO baseline result of 44.08 pb becomes 44.26 pb, a shift of  $+0.4\%$  (when only updated the splitting functions the respective value is 44.38 pb, i.e. a shift of  $0.7\%$ ). In the case of the VBF cross-sections, we have verified that the impact of the updated splitting functions is negligible, i.e. of order  $0.1\%$ . Therefore, the difference between the central predictions of the aN<sup>3</sup>LO fits of NNPDF and MSHT is reduced by around  $1\%$  when the same parametrization of splitting functions from [19] is used. However, the average value obtained from a combined set of PDFs is almost unchanged. Moreover, because the updated PDFs get closer, the uncertainty found with this updated combination is reduced, consistent with the reduction in theoretical uncertainty due to better knowledge of N<sup>3</sup>LO splitting functions and transition matrix elements. In summary, the updated combination leads to an almost identical central prediction and a somewhat reduced uncertainty.

Hence, we conclude that the results using the combination presented here, based on published PDF sets, can currently be relied upon to produce a reliable set of predictions and a conservative uncertainty estimate. Similarly, the individual published aN<sup>3</sup>LO PDF sets can be taken to be reliable, as updated information results in very similar predictions well within the uncertainty, which again can be taken as conservative as improved N<sup>3</sup>LO knowledge would reduce theoretical uncertainty. On the other hand, we conclude that adopting a common set of N<sup>3</sup>LO splitting function does improve the overall consistency between the MSHT20 and NNPDF4.0 aN<sup>3</sup>LO sets, especially for the gluon-gluon luminosity. As more information on N<sup>3</sup>LO terms becomes available, it will be incorporated in future PDF sets, and PDFs based on common settings could be considered for future combinations. For the time being the existing sets may be reliably used, until they will be replaced by some newer version including updates based on improvements in N<sup>3</sup>LO knowledge but also potentially on increased data and other methodological changes.

## 5 Conclusion

In this note we have shown that the use of aN<sup>3</sup>LO PDFs is mandatory for accurate N<sup>3</sup>LO phenomenology at the LHC, focusing on the case of Higgs production cross-sections. For Higgs production in gluon fusion and in vector boson fusion the impact of switching from NNLO to aN<sup>3</sup>LO PDFs is rather larger than the PDF uncertainty, and also larger (for VBF much larger) than the difference between different PDF sets. Indeed, we have shown that differences between existing aN<sup>3</sup>LO PDF sets are moderate, and generally smaller than the difference between NNLO and aN<sup>3</sup>LO. We have verified that updates due to improved knowledge of N<sup>3</sup>LO splitting functions and transition matrix elements does not alter this conclusion.

Our results illustrate the limitations of N<sup>3</sup>LO phenomenology at the LHC using NNLO PDFs. In order to deal with these limitations, we have constructed combined aN<sup>3</sup>LO PDF sets, both pure QCD and QCD+QED, which allow for the computation of phenomenological predictions with a more conservative estimate of the uncertainty, as is appropriate when combining predictions that are not fully compatible. Clearly, a full N<sup>3</sup>LO PDF determination will only be possible once all processes currently used for PDF determination are known at this order, which is likely to take some time. In particular, the calculation of the massive corrections to the DIS coefficient functions and the full set of N<sup>3</sup>LO corrections to hadronic processes will almost certainly take many years to compute. In the meantime, our results clearly demonstrate that the available aN<sup>3</sup>LO PDFs represent the most accurate option for the deployment of N<sup>3</sup>LO calculations for LHC physics.

The MSHT20xNNPDF40\_an3lo and MSHT20xNNPDF40\_an3lo\_qed PDF sets presented in this note have been submitted to the LHAPDF repository [64]. They are also made available (alongside the corresponding NNLO baseline sets) at the link:

<https://zenodo.org/records/13843626>.

## Acknowledgments

We thank the convenors of Working Group 1 of the LHC Higgs Cross-Section Working Group (LHCHXSWG), in particular the gluon-fusion subgroup, for constructive feedback on the first draft of this document. We are also grateful to Amanda Cooper-Sarkar for questions and critical input, and members of the CT collaboration, in particular Joey Huston and Pavel Nadolsky, for discussion concerning N<sup>3</sup>LO PDFs and their uncertainties.

S. F. performed this work in part at the Aspen Center for Physics, which is supported by National Science Foundation Grant PHY-2210452, and is partially supported by an Italian PRIN2022 grant. R. D. B., L. D. D. and R. S. thank the Science and Technology Facilities Council (STFC) for support via grant awards ST/T000600/1 and ST/X000494/1. L. H.-L. and R. S. T. thank the Science and Technology Facilities Council (STFC) for support via grant awards ST/T000856/1 and ST/X000516/1. T. C. acknowledges that this project has received funding from the European Research Council (ERC) under the European Union’s Horizon 2020 research and innovation programme (Grant agreement No. 101002090 COLORFREE). E. R. N. is supported by the Italian Ministry of University and Research (MUR) through the “Rita Levi-Montalcini” Program. F. H. is supported by the Academy of Finland project 358090 and is funded as a part of the Center of Excellence in Quark Matter of the Academy of Finland, project 346326. M.U. is supported by the European Research Council under the European Union’s Horizon 2020 research and innovation Programme (grant agreement n.950246), and partially by the STFC consolidated grant ST/T000694/1 and ST/X000664/1.

## References

- [1] S. Bailey, T. Cridge, L. A. Harland-Lang, A. D. Martin, and R. S. Thorne, *Parton distributions from LHC, HERA, Tevatron and fixed target data: MSHT20 PDFs*, *Eur. Phys. J. C* **81** (2021), no. 4 341, [[arXiv:2012.04684](https://arxiv.org/abs/2012.04684)].
- [2] **NNPDF** Collaboration, R. D. Ball et al., *The path to proton structure at 1% accuracy*, *Eur. Phys. J. C* **82** (2022), no. 5 428, [[arXiv:2109.02653](https://arxiv.org/abs/2109.02653)].
- [3] J. McGowan, T. Cridge, L. A. Harland-Lang, and R. S. Thorne, *Approximate N<sup>3</sup>LO parton distribution functions with theoretical uncertainties: MSHT20aN<sup>3</sup>LO PDFs*, *Eur. Phys. J. C* **83** (2023), no. 3 185, [[arXiv:2207.04739](https://arxiv.org/abs/2207.04739)]. [Erratum: *Eur.Phys.J.C* 83, 302 (2023)].
- [4] **NNPDF** Collaboration, R. D. Ball et al., *The path to N<sup>3</sup>LO parton distributions*, *Eur. Phys. J. C* **84** (2024), no. 7 659, [[arXiv:2402.18635](https://arxiv.org/abs/2402.18635)].
- [5] T. Cridge, L. A. Harland-Lang, and R. S. Thorne, *Combining QED and approximate N<sup>3</sup>LO QCD corrections in a global PDF fit: MSHT20qed\_an3lo PDFs*, *SciPost Phys.* **17** (2024), no. 1 026, [[arXiv:2312.07665](https://arxiv.org/abs/2312.07665)].
- [6] A. Barontini, N. Laurenti, and J. Rojo, *NNPDF4.0 aN<sup>3</sup>LO PDFs with QED corrections*, in *31st International Workshop on Deep-Inelastic Scattering and Related Subjects*, 6, 2024. [arXiv:2406.01779](https://arxiv.org/abs/2406.01779).
- [7] S. Moch, B. Ruijl, T. Ueda, J. A. M. Vermaseren, and A. Vogt, *Four-Loop Non-Singlet Splitting Functions in the Planar Limit and Beyond*, *JHEP* **10** (2017) 041, [[arXiv:1707.08315](https://arxiv.org/abs/1707.08315)].
- [8] J. Davies, A. Vogt, B. Ruijl, T. Ueda, and J. A. M. Vermaseren, *Large-n<sub>f</sub> contributions to the four-loop splitting functions in QCD*, *Nucl. Phys. B* **915** (2017) 335–362, [[arXiv:1610.07477](https://arxiv.org/abs/1610.07477)].
- [9] T. Gehrmann, A. von Manteuffel, V. Sotnikov, and T.-Z. Yang, *Complete N<sub>f</sub><sup>2</sup> contributions to four-loop pure-singlet splitting functions*, *JHEP* **01** (2024) 029, [[arXiv:2308.07958](https://arxiv.org/abs/2308.07958)].
- [10] T. Gehrmann, A. von Manteuffel, V. Sotnikov, and T.-Z. Yang, *The N<sub>f</sub>C<sub>F</sub><sup>3</sup> contribution to the non-singlet splitting function at four-loop order*, *Phys. Lett. B* **849** (2024) 138427, [[arXiv:2310.12240](https://arxiv.org/abs/2310.12240)].
- [11] G. Falcioni, F. Herzog, S. Moch, J. Vermaseren, and A. Vogt, *The double fermionic contribution to the four-loop quark-to-gluon splitting function*, *Phys. Lett. B* **848** (2024) 138351, [[arXiv:2310.01245](https://arxiv.org/abs/2310.01245)].

- [12] S. Moch, B. Ruijl, T. Ueda, J. A. M. Vermaseren, and A. Vogt, *On quartic colour factors in splitting functions and the gluon cusp anomalous dimension*, *Phys. Lett. B* **782** (2018) 627–632, [[arXiv:1805.09638](https://arxiv.org/abs/1805.09638)].
- [13] S. Moch, B. Ruijl, T. Ueda, J. A. M. Vermaseren, and A. Vogt, *Low moments of the four-loop splitting functions in QCD*, *Phys. Lett. B* **825** (2022) 136853, [[arXiv:2111.15561](https://arxiv.org/abs/2111.15561)].
- [14] G. Falcioni, F. Herzog, S. Moch, and A. Vogt, *Four-loop splitting functions in QCD – The quark-quark case*, *Phys. Lett. B* **842** (2023) 137944, [[arXiv:2302.07593](https://arxiv.org/abs/2302.07593)].
- [15] G. Falcioni, F. Herzog, S. Moch, and A. Vogt, *Four-loop splitting functions in QCD – The gluon-to-quark case*, *Phys. Lett. B* **846** (2023) 138215, [[arXiv:2307.04158](https://arxiv.org/abs/2307.04158)].
- [16] S. Moch, B. Ruijl, T. Ueda, J. Vermaseren, and A. Vogt, *Additional moments and  $x$ -space approximations of four-loop splitting functions in QCD*, *Phys. Lett. B* **849** (2024) 138468, [[arXiv:2310.05744](https://arxiv.org/abs/2310.05744)].
- [17] G. Falcioni, F. Herzog, S. Moch, A. Pelloni, and A. Vogt, *Four-loop splitting functions in QCD – The quark-to-gluon case*, *Phys. Lett. B* **856** (2024) 138906, [[arXiv:2404.09701](https://arxiv.org/abs/2404.09701)].
- [18] G. Falcioni, F. Herzog, S. Moch, and S. Van Thuren, *Constraints for twist-two alien operators in QCD*, [arXiv:2409.02870](https://arxiv.org/abs/2409.02870).
- [19] G. Falcioni, F. Herzog, S. Moch, A. Pelloni, and A. Vogt, *Four-loop splitting functions in QCD – The gluon-gluon case* –, [arXiv:2410.08089](https://arxiv.org/abs/2410.08089).
- [20] H. Kawamura, N. A. Lo Presti, S. Moch, and A. Vogt, *On the next-to-next-to-leading order QCD corrections to heavy-quark production in deep-inelastic scattering*, *Nucl. Phys. B* **864** (2012) 399–468, [[arXiv:1205.5727](https://arxiv.org/abs/1205.5727)].
- [21] I. Bierenbaum, J. Blümlein, and S. Klein, *Mellin Moments of the  $O(\alpha_s^3)$  Heavy Flavor Contributions to unpolarized Deep-Inelastic Scattering at  $Q^2 \gg m^2$  and Anomalous Dimensions*, *Nucl. Phys. B* **820** (2009) 417–482, [[arXiv:0904.3563](https://arxiv.org/abs/0904.3563)].
- [22] J. Ablinger, A. Behring, J. Blümlein, A. De Freitas, A. Hasselhuhn, A. von Manteuffel, M. Round, C. Schneider, and F. Wißbrock, *The 3-Loop Non-Singlet Heavy Flavor Contributions and Anomalous Dimensions for the Structure Function  $F_2(x, Q^2)$  and Transversity*, *Nucl. Phys. B* **886** (2014) 733–823, [[arXiv:1406.4654](https://arxiv.org/abs/1406.4654)].
- [23] J. Ablinger, A. Behring, J. Blümlein, A. De Freitas, A. von Manteuffel, and C. Schneider, *The 3-loop pure singlet heavy flavor contributions to the structure function  $F_2(x, Q^2)$  and the anomalous dimension*, *Nucl. Phys. B* **890** (2014) 48–151, [[arXiv:1409.1135](https://arxiv.org/abs/1409.1135)].
- [24] J. Blümlein, P. Marquard, C. Schneider, and K. Schönwald, *The three-loop unpolarized and polarized non-singlet anomalous dimensions from off shell operator matrix elements*, *Nucl. Phys. B* **971** (2021) 115542, [[arXiv:2107.06267](https://arxiv.org/abs/2107.06267)].
- [25] J. Ablinger, J. Blümlein, A. De Freitas, A. Hasselhuhn, A. von Manteuffel, M. Round, and C. Schneider, *The  $O(\alpha_s^3 T_F^2)$  Contributions to the Gluonic Operator Matrix Element*, *Nucl. Phys. B* **885** (2014) 280–317, [[arXiv:1405.4259](https://arxiv.org/abs/1405.4259)].
- [26] J. Ablinger, J. Blümlein, A. De Freitas, A. Hasselhuhn, A. von Manteuffel, M. Round, and C. Schneider, *3-loop Massive  $O(T_F^2)$  Contributions to the DIS Operator Matrix Element  $A_{gg}$* , *Nucl. Part. Phys. Proc.* **258-259** (2015) 37–40, [[arXiv:1409.1435](https://arxiv.org/abs/1409.1435)].
- [27] J. Ablinger, J. Blümlein, A. De Freitas, A. Hasselhuhn, A. von Manteuffel, M. Round, C. Schneider, and F. Wißbrock, *The transition matrix element  $A_{gq}(N)$  of the variable flavor number scheme at  $O(\alpha s^3)$* , *Nuclear Physics B* **882** (May, 2014) 263–288, [[arXiv:1402.0359](https://arxiv.org/abs/1402.0359)].
- [28] J. Ablinger, A. Behring, J. Blümlein, A. De Freitas, A. Goedelke, A. von Manteuffel, C. Schneider, and K. Schönwald, *The unpolarized and polarized single-mass three-loop heavy flavor operator matrix elements  $A_{gg,Q}$  and  $\Delta A_{gg,Q}$* , *JHEP* **12** (2022) 134, [[arXiv:2211.05462](https://arxiv.org/abs/2211.05462)].

[29] J. Ablinger, A. Behring, J. Blümlein, A. De Freitas, A. von Manteuffel, C. Schneider, and K. Schönwald, *The first-order factorizable contributions to the three-loop massive operator matrix elements  $AQg(3)$  and  $\Delta AQg(3)$* , *Nucl. Phys. B* **999** (2024) 116427, [[arXiv:2311.00644](https://arxiv.org/abs/2311.00644)].

[30] J. Ablinger, A. Behring, J. Blümlein, A. De Freitas, A. von Manteuffel, C. Schneider, and K. Schönwald, *The non-first-order-factorizable contributions to the three-loop single-mass operator matrix elements  $A_{Qg}^{(3)}$  and  $\Delta A_{Qg}^{(3)}$* , [arXiv:2403.00513](https://arxiv.org/abs/2403.00513).

[31] J. A. M. Vermaseren, A. Vogt, and S. Moch, *The third-order QCD corrections to deep-inelastic scattering by photon exchange*, *Nucl. Phys. B* **724** (2005) 3, [[hep-ph/0504242](https://arxiv.org/abs/hep-ph/0504242)].

[32] J. Blümlein, P. Marquard, C. Schneider, and K. Schönwald, *The massless three-loop Wilson coefficients for the deep-inelastic structure functions  $F_2$ ,  $F_L$ ,  $xF_3$  and  $g_1$* , *JHEP* **11** (2022) 156, [[arXiv:2208.14325](https://arxiv.org/abs/2208.14325)].

[33] F. Caola, W. Chen, C. Duhr, X. Liu, B. Mistlberger, F. Petriello, G. Vita, and S. Weinzierl, *The Path forward to  $N^3LO$* , in *Snowmass 2021*, 3, 2022. [arXiv:2203.06730](https://arxiv.org/abs/2203.06730).

[34] C. Duhr, F. Dulat, and B. Mistlberger, *Charged current Drell-Yan production at  $N^3LO$* , *JHEP* **11** (2020) 143, [[arXiv:2007.13313](https://arxiv.org/abs/2007.13313)].

[35] C. Duhr, F. Dulat, and B. Mistlberger, *Drell-Yan Cross Section to Third Order in the Strong Coupling Constant*, *Phys. Rev. Lett.* **125** (2020), no. 17 172001, [[arXiv:2001.07717](https://arxiv.org/abs/2001.07717)].

[36] C. Duhr and B. Mistlberger, *Lepton-pair production at hadron colliders at  $N^3LO$  in QCD*, *JHEP* **03** (2022) 116, [[arXiv:2111.10379](https://arxiv.org/abs/2111.10379)].

[37] X. Chen, T. Gehrmann, N. Glover, A. Huss, T.-Z. Yang, and H. X. Zhu, *Dilepton Rapidity Distribution in Drell-Yan Production to Third Order in QCD*, *Phys. Rev. Lett.* **128** (2022), no. 5 052001, [[arXiv:2107.09085](https://arxiv.org/abs/2107.09085)].

[38] R. D. Ball, S. Carrazza, L. Del Debbio, S. Forte, J. Gao, et al., *Parton Distribution Benchmarking with LHC Data*, *JHEP* **1304** (2013) 125, [[arXiv:1211.5142](https://arxiv.org/abs/1211.5142)].

[39] R. D. Ball and R. L. Pearson, *Correlation of theoretical uncertainties in PDF fits and theoretical uncertainties in predictions*, *Eur. Phys. J. C* **81** (2021), no. 9 830, [[arXiv:2105.05114](https://arxiv.org/abs/2105.05114)].

[40] J. Davies, C. H. Kom, S. Moch, and A. Vogt, *Resummation of small- $x$  double logarithms in QCD: inclusive deep-inelastic scattering*, *JHEP* **08** (2022) 135, [[arXiv:2202.10362](https://arxiv.org/abs/2202.10362)].

[41] J. Andersen et al., *Les Houches 2023: Physics at TeV Colliders: Standard Model Working Group Report*, in *Physics of the TeV Scale and Beyond the Standard Model: Intensifying the Quest for New Physics*, 6, 2024. [arXiv:2406.00708](https://arxiv.org/abs/2406.00708).

[42] A. Cooper-Sarkar, T. Cridge, F. Giuli, L. A. Harland-Lang, F. Hekhorn, J. Huston, G. Magni, S. Moch, and R. S. Thorne, *A Benchmarking of QCD Evolution at Approximate  $N^3LO$* , [arXiv:2406.16188](https://arxiv.org/abs/2406.16188).

[43] R. S. Thorne, T. Cridge, and L. Harland-Lang, *MSHT Updates 2024*, in *31st International Workshop on Deep-Inelastic Scattering and Related Subjects*, 8, 2024. [arXiv:2408.10008](https://arxiv.org/abs/2408.10008).

[44] R. Thorne, <https://indico.cern.ch/event/1435677/contributions/6133441/attachments/2977567/5242015/PDF4LHC2024.pdf>, . “MSHT PDF Update”, PDF4LHC Workshop 2024.

[45] T. Cridge, <https://indico.cern.ch/event/1436959/contributions/6352248/author/9387795>, . ”Combination of aN3LO PDFs and implications for Higgs production cross-sections at the LHC”, DIS2025.

[46] G. Magni, [https://indico.cern.ch/event/1435677/contributions/6246030/attachments/2977793/5242448/PDF4LHC\\_an3lo\\_02\\_12\\_24.pdf](https://indico.cern.ch/event/1435677/contributions/6246030/attachments/2977793/5242448/PDF4LHC_an3lo_02_12_24.pdf), . “Combination of aN3LO PDFs and implications for Higgs production”, PDF4LHC Workshop 2024.

[47] J. Baglio, C. Duhr, B. Mistlberger, and R. Szafron, *Inclusive production cross sections at  $N^3LO$* , *JHEP* **12** (2022) 066, [[arXiv:2209.06138](https://arxiv.org/abs/2209.06138)].

[48] C. Anastasiou, C. Duhr, F. Dulat, E. Furlan, T. Gehrmann, F. Herzog, A. Lazopoulos, and B. Mistlberger, *High precision determination of the gluon fusion Higgs boson cross-section at the LHC*, *JHEP* **05** (2016) 058, [[arXiv:1602.00695](https://arxiv.org/abs/1602.00695)].

[49] J. Butterworth et al., *PDF4LHC recommendations for LHC Run II*, *J. Phys. G* **43** (2016) 023001, [[arXiv:1510.03865](https://arxiv.org/abs/1510.03865)].

[50] **NNPDF** Collaboration, R. D. Ball et al., *Determination of the theory uncertainties from missing higher orders on NNLO parton distributions with percent accuracy*, *Eur. Phys. J. C* **84** (2024), no. 5 517, [[arXiv:2401.10319](https://arxiv.org/abs/2401.10319)].

[51] **PDF4LHC Working Group** Collaboration, R. D. Ball et al., *The PDF4LHC21 combination of global PDF fits for the LHC Run III*, *J. Phys. G* **49** (2022), no. 8 080501, [[arXiv:2203.05506](https://arxiv.org/abs/2203.05506)].

[52] **PDF4LHC21 combination group** Collaboration, T. Cridge, *PDF4LHC21: Update on the benchmarking of the CT, MSHT and NNPDF global PDF fits*, *SciPost Phys. Proc.* **8** (2022) 101, [[arXiv:2108.09099](https://arxiv.org/abs/2108.09099)].

[53] J. Erler and R. Ferro-Hernández, *Alternative to the application of PDG scale factors*, *Eur. Phys. J. C* **80** (2020), no. 6 541, [[arXiv:2004.01219](https://arxiv.org/abs/2004.01219)].

[54] **LHC Higgs Cross Section Working Group** Collaboration, S. Dittmaier et al., *Handbook of LHC Higgs Cross Sections: 1. Inclusive Observables*, [arXiv:1101.0593](https://arxiv.org/abs/1101.0593).

[55] S. Carrazza, J. I. Latorre, J. Rojo, and G. Watt, *A compression algorithm for the combination of PDF sets*, *Eur. Phys. J. C* **75** (2015) 474, [[arXiv:1504.06469](https://arxiv.org/abs/1504.06469)].

[56] G. Watt and R. S. Thorne, *Study of Monte Carlo approach to experimental uncertainty propagation with MSTW 2008 PDFs*, *JHEP* **1208** (2012) 052, [[arXiv:1205.4024](https://arxiv.org/abs/1205.4024)].

[57] R. D. Ball, S. Forte, and R. Stegeman, *Correlation and combination of sets of parton distributions*, *Eur. Phys. J. C* **81** (2021), no. 11 1046, [[arXiv:2110.08274](https://arxiv.org/abs/2110.08274)].

[58] **NNPDF** Collaboration, R. D. Ball et al., *Photons in the proton: implications for the LHC*, [arXiv:2401.08749](https://arxiv.org/abs/2401.08749).

[59] M. Bonvini, R. D. Ball, S. Forte, S. Marzani, and G. Ridolfi, *Updated Higgs cross section at approximate  $N^3LO$* , *J. Phys. G* **41** (2014) 095002, [[arXiv:1404.3204](https://arxiv.org/abs/1404.3204)].

[60] M. Bonvini, *An approximate  $N^3LO$  cross section for Higgs production in gluon fusion*, *EPJ Web Conf.* **60** (2013) 12008, [[arXiv:1306.6633](https://arxiv.org/abs/1306.6633)].

[61] F. A. Dreyer and A. Karlberg, *Vector-Boson Fusion Higgs Production at Three Loops in QCD*, *Phys. Rev. Lett.* **117** (2016), no. 7 072001, [[arXiv:1606.00840](https://arxiv.org/abs/1606.00840)].

[62] F. A. Dreyer and A. Karlberg, *Vector-Boson Fusion Higgs Pair Production at  $N^3LO$* , *Phys. Rev. D* **98** (2018), no. 11 114016, [[arXiv:1811.07906](https://arxiv.org/abs/1811.07906)].

[63] S. Forte, A. Isgrò, and G. Vita, *Do we need  $N^3LO$  Parton Distributions?*, *Phys. Lett. B* **731** (2014) 136–140, [[arXiv:1312.6688](https://arxiv.org/abs/1312.6688)].

[64] A. Buckley, J. Ferrando, S. Lloyd, K. Nordström, B. Page, et al., *LHAPDF6: parton density access in the LHC precision era*, *Eur. Phys. J. C* **75** (2015) 132, [[arXiv:1412.7420](https://arxiv.org/abs/1412.7420)].